Defense Threat Reduction Agency
8725 John J. Kingman Road, MS-6201
Fort Belvoir, VA 22060-6201

DTRA-TR-15-008

TECHNICAL REPORT

Analysis of Air Activity Concentration Data Collected in the Kanto Plain, Japan, following the 2011 Fukushima Daiichi Nuclear Accident

June 2015

Prepared by:

Operation Tomodachi Registry,
Dose Assessment and Recording Working Group

For:

Assistant Secretary of Defense for Health Affairs

DESTRUCTION NOTICE:

Destroy this report when it is no longer needed.
Do not return to sender.

PLEASE NOTIFY THE DEFENSE THREAT REDUCTION AGENCY, ATTN: DTRIAC/ J9STT, 8725 JOHN J. KINGMAN ROAD, MS-6201, FT BELVOIR, VA 22060-6201, IF YOUR ADDRESS IS INCORRECT, IF YOU WISH THAT IT BE DELETED FROM THE DISTRIBUTION LIST, OR IF THE ADDRESSEE IS NO LONGER EMPLOYED BY YOUR ORGANIZATION.

This page intentionally left blank.

REPORT DOCUMENTATION PAGE

Form Approved
OMB No. 0704-0188

1. REPORT DATE *(DD-MM-YYYY)*	2. REPORT TYPE	3. DATES COVERED *(From - To)*
09-06-2015	TECHNICAL	

4. TITLE AND SUBTITLE
Analysis of Air Activity Concentration Data Collected in the Kanto Plain, Japan, following the 2011 Fukushima Daiichi Nuclear Accident

5a. CONTRACT NUMBER
HDTRA1-15-C-0002

5b. GRANT NUMBER

5c. PROGRAM ELEMENT NUMBER

6. AUTHOR(S)
Singer, Harvey A.

5d. PROJECT NUMBER

5e. TASK NUMBER

5f. WORK UNIT NUMBER

7. PERFORMING ORGANIZATION NAME(S) AND ADDRESS(ES)
George Mason University, Fairfax, VA and Leidos, Alexandria, VA

8. PERFORMING ORGANIZATION REPORT NUMBER

9. SPONSORING/MONITORING AGENCY NAME(S) AND ADDRESS(ES)
Nuclear Technology Department, Attn: Dr. Blake
Defense Threat Reduction Agency
8725 John J. Kingman Road, Mail Stop 6201
Fort Belvoir, VA 22060-6201

10. SPONSOR/MONITOR'S ACRONYM(S)
DTRA J9-NTSN

11. SPONSORING/MONITORING AGENCY REPORT NUMBER
DTRA-TR-15-008

12. DISTRIBUTION AVAILABILITY STATEMENT
DISTRIBUTION A. Approved for public release: distribution is unlimited.

13. SUPPLEMENTARY NOTES

14. ABSTRACT
A novel use of econometric analysis was applied for the comparison of time series of air sampling data considered for use in dose assessments of DOD participants in Operation Tomodachi. Autocorrelation analysis was used to explore the time structure of the data and cointegration was used to determine whether or not the time series were co-trended with each other. These methods are applied to time series of air activity concentration collected at three locations following the release of radioactive materials from the Fukushima Daiichi Nuclear Power Station. The time series at Yokota Air Base and the International Monitoring Station are shown to have similar time structure and behavior and can be cointegrated with each other, while those at Yokosuka Naval Base were very different. The results support decisions on data used in dose assessments and suggest the methods may be useful in other similar exposure situations.

15. SUBJECT TERMS
Operation Tomodachi, Department of Defense, Japan, Fukushima, accidents, nuclear; analysis, statistical; emissions, atmospheric; radioactivity, airborne

16. SECURITY CLASSIFICATION OF:			17. LIMITATION OF ABSTRACT	18. NUMBER OF PAGES	19a. NAME OF RESPONSIBLE PERSON
a. REPORT	b. ABSTRACT	c. THIS PAGE			Paul K. Blake, PhD
U		U	U	50 Pages	19b. TELEPONE NUMBER (*Include area code)* (703) 767-3433

UNIT CONVERSION TABLE

U.S. customary units to and from international units of measurement*

U.S. Customary Units	Multiply by → / ← Divide by†		International Units
Length/Area/Volume			
inch (in)	2.54	$\times 10^{-2}$	meter (m)
foot (ft)	3.048	$\times 10^{-1}$	meter (m)
yard (yd)	9.144	$\times 10^{-1}$	meter (m)
mile (mi, international)	1.609 344	$\times 10^{3}$	meter (m)
mile (nmi, nautical, U.S.)	1.852	$\times 10^{3}$	meter (m)
barn (b)	1	$\times 10^{-28}$	square meter (m^2)
gallon (gal, U.S. liquid)	3.785 412	$\times 10^{-3}$	cubic meter (m^3)
cubic foot (ft^3)	2.831 685	$\times 10^{-2}$	cubic meter (m^3)
Mass/Density			
pound (lb)	4.535 924	$\times 10^{-1}$	kilogram (kg)
atomic mass unit (AMU)	1.660 539	$\times 10^{-27}$	kilogram (kg)
pound-mass per cubic foot (lb ft^{-3})	1.601 846	$\times 10^{1}$	kilogram per cubic meter (kg m^{-3})
Pound-force (lbf avoirdupois)	4.448 222		Newton (N)
Energy/Work/Power			
electronvolt (eV)	1.602 177	$\times 10^{-19}$	joule (J)
erg	1	$\times 10^{-7}$	joule (J)
kiloton (kT) (TNT equivalent)	4.184	$\times 10^{12}$	joule (J)
British thermal unit (Btu) (thermochemical)	1.054 350	$\times 10^{3}$	joule (J)
foot-pound-force (ft lbf)	1.355 818		joule (J)
calorie (cal) (thermochemical)	4.184		joule (J)
Pressure			
atmosphere (atm)	1.013 250	$\times 10^{5}$	pascal (Pa)
pound force per square inch (psi)	6.984 757	$\times 10^{3}$	pascal (Pa)
Temperature			
degree Fahrenheit (^oF)	$[T(^oF) - 32]/1.8$		degree Celsius (^oC)
degree Fahrenheit (^oF)	$[T(^oF) + 459.67]/1.8$		kelvin (K)
Radiation			
activity of radionuclides [curie (Ci)]	3.7	$\times 10^{10}$	per second (s^{-1}‡)
air exposure [roentgen (R)]	2.579 760	$\times 10^{-4}$	coulomb per kilogram (C kg^{-1})
absorbed dose (rad)	1	$\times 10^{-2}$	joule per kilogram (J kg^{-1}§)
equivalent and effective dose (rem)	1	$\times 10^{-2}$	joule per kilogram (J kg^{-1}**)

*Specific details regarding the implementation of SI units may be viewed at http://www.bipm.org/en/si/.

†Multiply the U.S. customary unit by the factor to get the international unit. Divide the international unit by the factor to get the U.S. customary unit.

‡The special name for the SI unit of the activity of a radionuclide is the becquerel (Bq). (1 Bq = 1 s^{-1}).

§The special name for the SI unit of absorbed dose is the gray (Gy). (1 Gy = 1 J kg^{-1}).

**The special name for the SI unit of equivalent and effective dose is the sievert (Sv). (1 Sv = 1 J kg^{-1}).

DTRA-TR-15-008: Analysis of Air Activity Concentration Data Collected in the Kanto Plain, Japan, following the 2011 Fukushima Daiichi Nuclear Accident

Table of Contents

List of Figures ii

Acknowledgements v

Executive Summary vi

Section 1. Background and Introduction 1

Section 2. Graphical and Trend Analysis of the Data 4

Section 3. Time Series Comparisons: Methods and Results 8

3.1 Time Series Structure 8

3.2 Time Series Cointegration 13

3.3 Summary and Discussion 18

Section 4. Conclusions 19

Section 5. References 20

Appendix A. Plots of Air Concentration Data and Statistical Analysis Results 21

A-1. Time Series 22
A-2. Autocorrelation Functions 25
A-3. First Differences 30
A-4. Cointegration 33
A-5. Pairwise Differences 38

List of Figures

Figure 1. Location maps: a. Major U.S. military bases (red stars) and FDNPS (yellow trefoil), b. Map of the Kanto Plain on Honshu..... 2

Figure 2. Logarithmic values of Cs-134 air activity concentration for Yokota AB and IMS-Takasaki 5

Figure 3. Logarithmic values of Cs-134 air activity concentration for Yokosuka NB..... 6

Figure 4. ACF of the logarithmic values of Cs-134 air activity concentration for Yokota AB..... 9

Figure 5. ACF of the logarithmic values Cs-134 air activity concentration for IMS-Takasaki .. 10

Figure 6. ACF of the logarithmic values of Cs-134 air activity concentration for Yokosuka NB 11

Figure 7. First differences in logarithmic values of air activity concentrations of Cs-134 for Yokota AB and IMS-Takasaki..... 12

Figure 8. First differences in logarithmic values of Cs-134 air activity concentration at Yokosuka NB from March 21 to April 11 13

Figure 9. Cointegrating OLS relationship between Yokota AB and IMS-Takasaki for Cs-134 . 14

Figure 10. Cointegrating OLS relationship between Yokosuka NB and Yokota AB for Cs-134 15

Figure 11. Cointegrating OLS relationship between Yokosuka NB and IMS-Takasaki for Cs-134 16

Figure 12. Pairwise differences of the logarithmic values of air activity concentration for Cs-134 for the three locations..... 17

Figure A-1. Logarithmic values of I-131 air activity concentration for Yokota AB and IMS-Takasaki 22

Figure A-2. Logarithmic values of I-131 air activity concentration for Yokosuka NB 22

Figure A-3. Logarithmic values of Cs-134 air activity concentration for Yokota AB and IMS-Takasaki 23

Figure A-4. Logarithmic values of Cs-134 air activity concentration for Yokosuka NB..... 23

Figure A-5. Logarithmic values of Cs-137 air activity concentration for Yokota AB and IMS-Takasaki 24

Figure A-6. Logarithmic values of Cs-137 air activity concentration for Yokosuka NB..... 24

Figure A-7. ACF of the logarithmic values of I-131 air activity concentration for IMS-Takasaki 25

Figure A-8. ACF of the logarithmic values of Cs-134 air activity concentration for IMS-Takasaki 25

Figure A-9. ACF of the logarithmic values of Cs-137 air activity concentration for IMS-Takasaki 26

Figure A-10. ACF of the logarithmic values of I-131 air activity concentration for Yokota AB 26

Figure A-11. ACF of the logarithmic values of Cs-134 air activity concentration for Yokota AB 27
Figure A-12. ACF of the logarithmic values of Cs-137 air activity concentration for Yokota AB 27
Figure A-13. ACF of the logarithmic values of I-131 air activity concentration for Yokosuka NB 28
Figure A-14. ACF of the logarithmic values of Cs-134 air activity concentration for Yokosuka NB 28
Figure A-15. ACF of the logarithmic values of Cs-137 air activity concentration for Yokosuka NB 29
Figure A-16. First differences in logarithmic values of I-131 air activity concentration for Yokota AB and IMS-Takasaki 30
Figure A-17. First differences in logarithmic values of I-131 air activity concentration for Yokosuka NB 30
Figure A-18. First differences in logarithmic values of Cs-134 air activity concentration for Yokota AB and IMS-Takasaki 31
Figure A-19. First differences in logarithmic values of Cs-134 air activity concentration for Yokosuka NB 31
Figure A-20. First differences in logarithmic values of Cs-137 air activity concentration for Yokota AB and IMS-Takasaki 32
Figure A-21. First differences in logarithmic values of Cs-137 air activity concentration for Yokosuka NB 32
Figure A-22. Cointegrating OLS relationship between Yokota AB and IMS-Takasaki for I-131 33
Figure A-23. Cointegrating OLS relationship between Yokosuka NB and Yokota AB for I-131 33
Figure A-24. Cointegrating OLS relationship between Yokosuka NB and IMS-Takasaki for I-131 34
Figure A-25. Cointegrating OLS relationship between Yokota AB and IMS-Takasaki for Cs-134 34
Figure A-26. Cointegrating OLS relationship between Yokosuka NB and Yokota AB for Cs-134 35
Figure A-27. Cointegrating OLS relationship between Yokosuka NB and IMS-Takasaki for Cs-134 35
Figure A-28. Cointegrating OLS relationship between Yokota AB and IMS-Takasaki for Cs-137 36
Figure A-29. Cointegrating OLS relationship between Yokosuka NB and Yokota AB for Cs-137 36

Figure A-30. Cointegrating OLS relationship between Yokosuka NB and IMS-Takasaki for Cs-137 37
Figure A-31. Pairwise differences of the logarithmic values of air activity concentration for I-131 38
Figure A-32. Pairwise differences of the logarithmic values of air activity concentration for Cs-134 38
Figure A-33 . Pairwise differences of the logarithmic values of air activity concentration for Cs-137 39

Acknowledgements

The author gratefully acknowledges the support of the following:

- Dr. Mondher Chehata, Dr. David Case, Dr. Ronald Weitz, Mr. Michael McKenzie-Carter, CHP, and Dr. Steven Egbert, all at Leidos, Inc., for their valuable comments, critiques, and suggestions in reviewing previous drafts of this manuscript.
- The authors of radiation dose assessment reports prepared by the Operation Tomodachi Dose Assessment and Recording Working Group for bringing forth the problem and providing insights into the technical details.
- Dr. Jon W. Beard and Dr. Sidhartha Das, both of the School of Business of George Mason University, for their advice and many suggestions.
- Dr. T. Krishna Kumar, of Rockville Analytics and George Washington University, is especially thanked for suggesting cointegration as an approach.
- Dr. Paul Blake, of the Nuclear Technology Department, Defense Threat Reduction Agency, for his encouragement and support.

Executive Summary

Department of Defense affiliated individuals were potentially exposed to radiation as a result of the Fukushima Daiichi nuclear accident. Over 60 percent of the shore-based affiliated individuals were located on the Kanto Plain of the main island (Honshu) of Japan. Evaluations of air activity concentrations of radionuclides at several locations there raised concerns about the validity of their use in estimating radiation doses.

This technical report discusses a novel use of econometric analysis for the comparison of time series of air sampling data collected at three locations in the Kanto Plain area of Japan. The study was initiated to statistically compare time series of concentrations of airborne radioactive material released from the Fukushima Daiichi Nuclear Power Station, which was damaged as a result of the tsunami following the strong earthquake that occurred on March 11, 2011. The time series of concentrations at these locations were expected to exhibit similar characteristics, but plots of the data for one location were obviously dissimilar to plots of corresponding data for the other two locations. Specifically, this study was undertaken to determine whether the data at Yokosuka Naval Base were consistent with corresponding data measured at Yokota Air Base and the International Monitoring Station-Takasaki.

Because appropriate statistical methods could not be found in the health physics literature, some methods of econometrics were used. Two statistical methods in particular are described and applied to data in this report. First, autocorrelation analysis is used to explore and compare the time structure of the data. Second, cointegration is applied to determine if the time series are co-trended with one another. Based on these methods, the time series at Yokota Air Base and the International Monitoring Station-Takasaki are shown to have similar time structure and behavior and can be cointegrated with each other. These methods also demonstrate that the data for Yokosuka Naval Base are very different from those of the latter locations. They show different behavior and structure and the data cannot be cointegrated with the corresponding series from either of the other two locations. This analysis identified possible complications with the comparisons of Yokosuka time series with either of the other two, including the more limited nature of the Yokosuka data and possible effects attributed to geographical location. In contrast, these differences could be attributed to the episodic sampling at Yokosuka and the intentional selection of high-sided values.

This econometric analysis reinforces a conclusion stated in Cassata et al. (2012) that the air sampling data for Yokosuka Naval Base are deemed less reliable than the Yokota Air Base data for southern Kanto Plain military bases. The methods used here should be considered for use in other health physics studies where multiple time series are available, such as in some radiation dose assessments.

Section 1.

Background and Introduction

At 1446 Japan Standard Time on March 11, 2011, a 9.0 magnitude earthquake occurred 129 km (80 mi) east of Sendai and 372 km (231 mi) northeast of Tokyo off the coast of Honshu Island. The tsunami triggered by the earthquake damaged the Fukushima Daiichi Nuclear Power Station (FDNPS) causing radioactive materials to be released into the environment. These included intermittent large releases of radioactive fission products from the damaged reactors that entered the atmosphere as gases and aerosols, which were then transported in the air by the changing weather patterns across much of Japan's main island of Honshu as well as out to sea. Details of this event are reported in Cassata et al. (2012).

The Department of Defense (DOD) response to provide humanitarian assistance and disaster relief was called Operation Tomodachi (OT). Individuals supporting this effort, their dependents, and others physically in Japan at the time but not providing support to OT, collectively constitute the DOD-affiliated population of interest (POI), and were potentially exposed to radiation. Assessments of radiation exposures for the shore-based and the fleet-based populations are described in Cassata et al. (2012) and Marro et al. (2014), respectively.

Some of the inputs to the dose assessment process reported by Cassata et al. (2012) were radionuclide activity concentrations in the air, water, and soil that were collected by various agencies of the DOD, the Department of Energy, the Government of Japan, and others. Air activity concentrations were either used as reported or estimated for periods of time for which data were not available or when data were judged unreliable.

The air activity concentrations in the Kanto Plain located south of the FDNPS and in the vicinity of the Tokyo metropolitan area received particular attention. Based on the area's geography and the characteristics of atmospheric transport and dispersion following each release from the FDNPS, it would be expected that the activity concentrations of airborne radioactive materials throughout the Kanto Plain have similar patterns over time (Cassata et al., 2012). Analysts and peer reviewers who examined the measured and derived air concentrations in the Kanto Plain raised questions about the quality and validity of the reported data for three of five monitoring locations compared with the air concentration results from sampling at Yokota Air Base (AB). These three locations are Akasaka Press Center in Tokyo Prefecture, and Atsugi Naval Air Facility (NAF) and Yokosuka Naval Base (NB) in Kanagawa Prefecture. These three locations are 229, 258, and 266 km, respectively (142, 160, and 165 mi) southwest of the FDNPS, and Yokota AB is 240 km (149 mi) southwest (Cassata et al., 2012). Figure 1a (from Figure 2 of Cassata et al., 2012) provides a location map of this event.

Of these locations, attention has focused on Yokosuka NB where high values of activity concentrations in air were reported for the latter part of March and early April 2011. Measured activity concentrations were very often up to several orders of magnitude higher than those measured at both the International Monitoring Station (IMS) in Takasaki, Gunma Prefecture, and Yokota AB for similar dates. These monitor locations are shown in Figure 1b (from Figure 12 of Chehata et al., 2013).

Figure 1. Location maps: a. Major U.S. military bases (red stars) and FDNPS (yellow trefoil), b. Map of the Kanto Plain on Honshu

Furthermore, the measurements collected at the latter two locations appear to decrease similarly with time during the latter part of March and early April, while the Yokosuka NB measurements remained high with no obvious temporal trend; see Figures 23 and 24 of Cassata et al. (2012). The fixed monitoring sites at Yokota AB and IMS-Takasaki collected data before, during and after the T= 62 days spanning the period from March 12 to May 12, 2011, which is one day longer than the exposure period established in Cassata et al. (2012). Air samples were collected continuously for each 24-hour day using extremely high air flow rates and produced radionuclide concentrations using gamma-ray spectrometric analytical methods, which were augmented by measurements at analytical laboratories in the United States (Cassata et al., 2012). In contrast, field measurements at Yokosuka NB were made episodically at various times during each day of collection and collection volumes were limited, thereby reducing sensitivity (Cassata et al., 2012). Note that Yokota AB is located somewhat between the IMS-Takasaki site, approximately 66 km (41 mi) to the northwest, and Yokosuka NB, at a similar distance to the southeast (Cassata et al., 2012, Figure 48).

There are additional justifications for regarding data from Yokosuka NB with some doubt. First, both MEXT[1] and SPEEDI[2] dose rate data, though primarily influenced by ground-deposited radionuclides at later times, have very similar characteristics throughout the Kanto Plain monitoring stations with some of the response characteristics directly influenced by airborne activity. Second, Yokota AB and IMS-Takasaki air concentrations coincide well with some observations of external dose rate and specific radionuclide contributions to external dose at the Chiba accelerator site, which is east of the Tokyo metropolitan area and a substantial distance from Yokota AB. (Rademacher, 2013)

On this basis, the air concentrations throughout the Kanto Plain due to releases of airborne radioactive materials from the FDNPS reactors would be expected to have similar characteristics. From visual inspection of the time series plots it is apparent that the air

[1] Ministry of Education, Culture, Sports, Science and Technology of Japan
[2] System for Prediction of Environment Emergency Dose Information

concentrations at Yokota AB and IMS-Takasaki share similar characteristics. However, as remarked in Cassata et al. (2012) and discussed in Section 2, the air concentrations reported at Yokosuka NB are dissimilar to both Yokota AB and IMS-Takasaki. Specifically, high air concentrations were reported at Yokosuka NB in late March even though there were no contemporaneous increases in ground-deposited radionuclides. Moreover, there were no known releases from the FDNPS reactors that could be linked to the aforementioned reported high concentrations. As a result, Yokosuka NB air sampling data contradicts findings from SPEEDI stations and reactor release data (Rademacher, 2013). This reinforces the conclusion stated in Cassata et al. (2012) that the air sampling data for Yokosuka NB are deemed less reliable than Yokota AB data for southern Kanto Plain military bases.

The special study reported in this technical report investigates and discusses the analysis of the time series of air activity concentrations collected at Yokota AB, IMS-Takasaki, and Yokosuka NB in terms of how they are similar to or different from each other. The objective is to determine on a statistical basis whether the data from Yokosuka NB are consistent or not with the corresponding data from Yokota AB and IMS-Takasaki.

Section 2.

Graphical and Trend Analysis of the Data

Time series of daily values of air activity concentration of many radionuclides were used for calculating radiological doses as described in Cassata et al. (2012). Here, the time series for Yokota AB, Yokosuka NB, and IMS-Takasaki are studied and compared.

The data consist of air activity concentration values in units of microbecquerel per cubic meter ($\mu Bq\ m^{-3}$) for these three locations for iodine-131 (I-131), cesium-134 (Cs-134), and cesium-137 (Cs-137). The data for Yokota AB and IMS-Takasaki are measured daily values of air activity concentrations of the radionuclides in air samples, collected for 24 hours each day, from March 12 to May 12, 2011. The length of the Yokota AB time series is $T = 62$ days; the length of the IMS-Takasaki time series is $T = 61$ days because the measurement for March 14 is missing. Note that for all three radionuclides, the time series for Yokota AB and IMS-Takasaki appear to move together in the sense that the series appear to follow each other, as noted in Cassata et al. (2012). In particular, these data appear to be consistent with each other in terms of their level (time-varying magnitude), drift (fluctuations about the mean magnitude at various times), and trend. The offsets in individual peaks and valleys between the time series for these two locations may be due to the difference in the time standards used (Japan Standard Time and Coordinated Universal Time). On this basis, Cassata et al. (2012) concluded that the time series from these two locations and from Yokota AB in particular provide a credible representation of the air concentrations in the Kanto Plain and, therefore, can serve as surrogates for air concentrations at other locations.

At Yokosuka NB, air concentration values were available only for at most $T = 16$ days (for I-131; slightly less for Cs-134 and Cs-137) of the 22-day span from March 21 through April 11, 2011. Of these days, the measurements were conducted by different laboratories through different methods using different apparatus from those for Yokota AB and IMS-Takasaki (as already noted). Investigation has revealed that the data in the time series for Yokosuka NB are not measured daily values as for Yokota AB or IMS-Takasaki. Rather, these time series were assembled from available measurements by selection of the largest of the multiple field measurements taken on each day for which data were collected. This data selection procedure was adopted to maximize the calculated radiation dose. The resulting time series for all three radionuclides were used in this analysis as reported (other than a conversion to common units); in particular, the gaps were preserved (except where noted).

The air activity concentrations for the three locations are denoted by $C_{IMS}(t)$, $C_{YAB}(t)$, and $C_{YNB}(t)$ for IMS-Takasaki, Yokota AB, and Yokosuka NB throughout this report. Common logarithms, that is, logarithms to the base 10, are used to linearize the exponentially-decaying values of the air activity concentration data. The time variations in the activity concentrations are expected to have primarily resulted from radioactive decay and/or atmospheric transport and dispersion effects, which can both be modeled as exponential relationships (strictly so for radioactive decay, approximately so for transport and dispersion). Thus the air activity concentration at a particular location can be modeled as a decreasing exponential function in time. Taking logarithms of both sides converts this function into a linear relation. This

transformation has the secondary benefit of substantially reducing the time-variation of the variance of the data by making it approximately constant (or at least sufficiently "constant") so as not to violate a requirement in the ordinary least squares (OLS) regressions that follow. The time series of logarithmic (log) values of air activity concentrations for the three locations are denoted by $\log[C_{IMS}(t)]$, $\log[C_{YAB}(t)]$, and $\log[C_{YNB}(t)]$ for IMS-Takasaki, Yokota AB, and Yokosuka NB throughout this report.

Figure 2 displays the time series plots of the log values of Cs-134 for Yokota AB and for IMS-Takasaki. Figure 3 shows the time series plot of the Cs-134 log values for Yokosuka NB. These figures for Cs-134 are representative of the corresponding figures for I-131 and Cs-137 (see Appendix A-1).

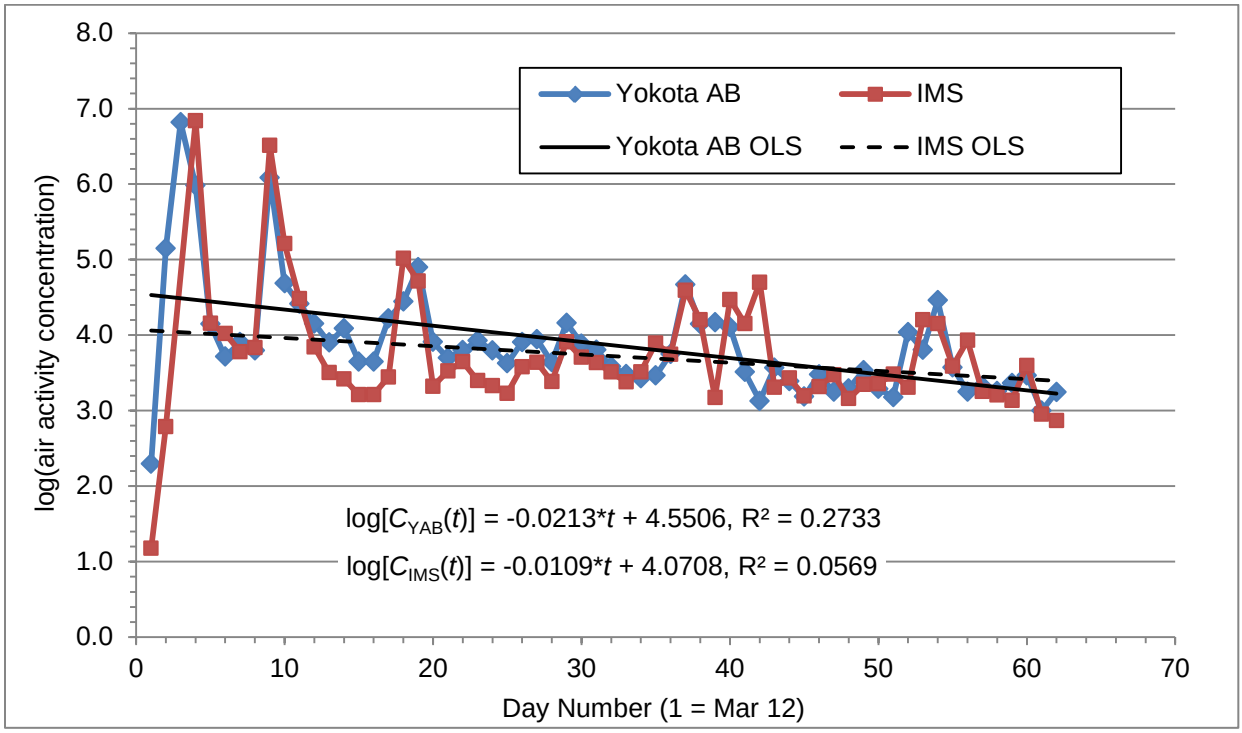

Figure 2. Logarithmic values of Cs-134 air activity concentration for Yokota AB and IMS-Takasaki

Also displayed on the graphs are the OLS fits regressed to the series. The coefficients of determination, R^2, are low for both Yokota AB and IMS-Takasaki. Although R^2 is the usual measure of "goodness-of-fit" of OLS regression, it is deceptive here, as is often the case with time series that periodically oscillate or episodically waiver around the regression line as here. However, that alone does not account for the observation that, visually, all the fits appear to be equally good. Here, R^2 by itself is not a good indicator of goodness-of-fit because of the radiological decay of the radionuclides. With regard to the data from IMS-Takasaki, the R^2 values for I-131, Cs-134, and Cs-137 are 0.51 (Figure A-1), 0.057 (Figure 2 and Figure A-3), and 0.050 (Figure A-5), respectively. On the basis of R^2 alone the fits are good for I-131 and poor for the cesium isotopes. The apparent discrepancy here is related to the half-lives of these isotopes, which are approximately 8 days for I-131, 2 years for Cs-134, and 30 years for Cs-137. In

particular, I-131 will decay almost completely over the measurement period, while the cesium isotopes will decay very little. As a result, the variation in the activity concentration values from radiological decay is large over this time interval for I-131 but small for the cesium isotopes. Thus, approximately 50% of the variation in log values is accounted for by the regression in time for I-131, compared to only about 5% for the cesium isotopes. It is not that the fits are not as good but rather that there is much less overall variation to account for with the much longer-lived cesium isotopes. Care must be taken here when making inferences regarding goodness-of-fit based on R^2 values alone.

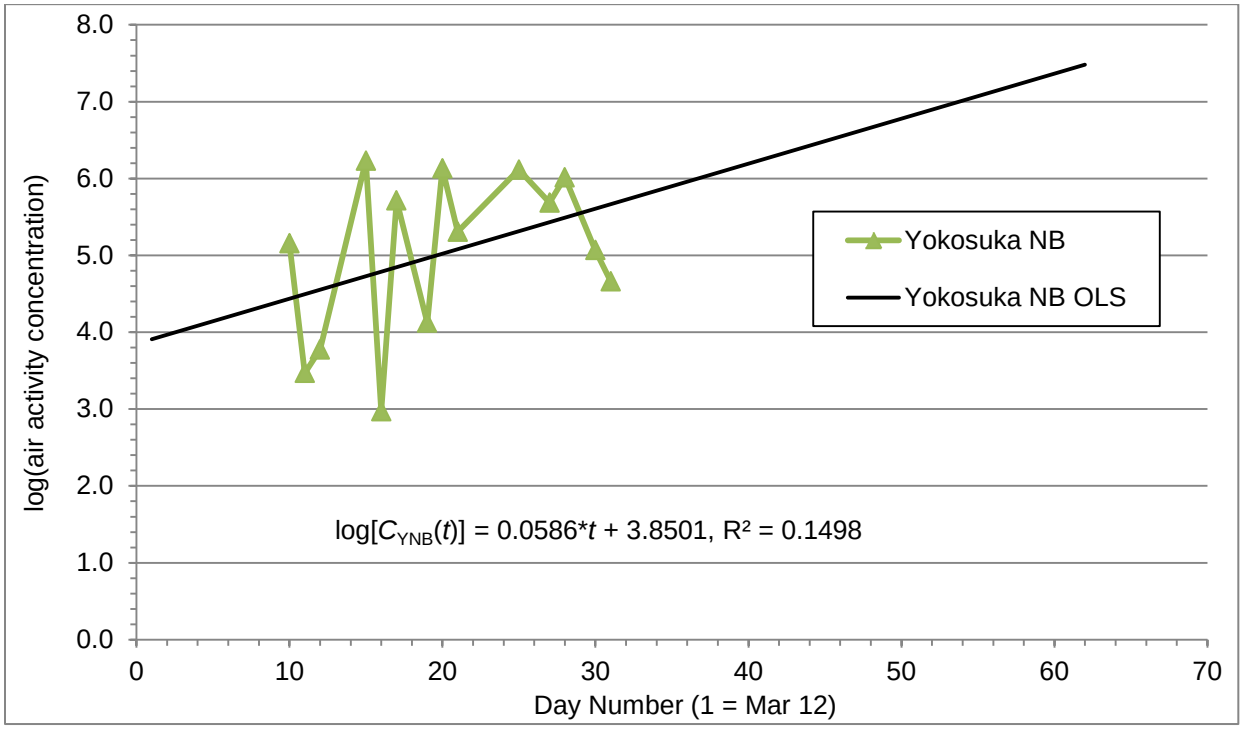

Figure 3. Logarithmic values of Cs-134 air activity concentration for Yokosuka NB

The log values of the series for IMS-Takasaki and Yokota AB decrease similarly in time along negative trends. This indicates that air concentrations decrease over time, as would be expected for radioactive decay and atmospheric transport and dispersion. Indeed, these two series appear to be nearly parallel to one another by virtue of the similarity in the numerical values of their slope parameters (the time coefficients). It appears that these time series are consistent with each other in that they appear to move together, i.e., that they are "co-trended." Also, these two series of log values appear to approach, eventually, the same long-run steady state level, such as if the time series had continued beyond the end of the measurement period. In econometrics, this behavior is referred to as cointegration, which is discussed in Section 3.2.

In contrast, the time series of log values of Cs-134 at Yokosuka NB (Figure 3) does not trend in a similar manner as the corresponding time series at either Yokota AB or IMS-Takasaki. As a result, this time series appears to be inconsistent with those from the other two locations. In particular, over the time period from March 21 to April 11 for which data are available for all three locations, the measured values are frequently orders of magnitude higher than the

corresponding values at both Yokota AB and IMS-Takasaki. Also, this time series does not possess the long-run behaviors (trends) of the time series at the other two locations nor does this series appear to converge to a long-run steady state level; instead it is oppositely directed along a positive trend. As a result, this series appears to remain high in level when the corresponding time series for IMS-Takasaki and Yokota AB both tend to decrease with time. The time series of Cs-134 log values at Yokosuka NB is not co-trended with the corresponding series from IMS-Takasaki and Yokota AB. The R^2 of this regression is also very low, but unlike the previous time series from IMS-Takasaki and Yokota AB, the fitted trend here is far less apparent. Consequently, results based on this regression must be viewed as equivocal. The comparisons shown here for Cs-134 are generally similar to those for I-131 and Cs-137 shown in Appendix A-1.

The co-trending behavior of the three time series of Cs-134 values is explored in Section 3.2 with the econometric concept of cointegration.

Section 3.

Time Series Comparisons: Methods and Results

Diagnostic statistical methods are used to determine the properties and structure of the time series of air activity concentrations at the three locations as a means of comparing them. The specific methods are time series structure and cointegration.

3.1 Time Series Structure

A stationary time series has the property that the mean, variance, and structure (in terms of its long-term behavior) do not change over time. Essentially, stationary time series appear "flat." Time series that do not exhibit these properties are nonstationary. In particular, time series that contain a trend are nonstationary. Note that nonstationarity is a more general statement than time-dependency. In addition to explicit dependence of the data upon time, nonstationarity includes the possibility that the statistical properties of the data (their mean and variance) may also vary with time. (Bowerman and O'Connell, 1993, Diebold, 2009; Hanke and Wichern, 2009; Madridakis et al., 1998; NIST/SEMATECH, 2015)

It is apparent from Figure 2 that the time series of log values of Cs-134 air activity concentrations for both Yokota AB and IMS-Takasaki are nonstationary. As already remarked, both time series have negative trends so that log values generally decrease with time. Moreover, the trends are similar (i.e., similar slopes) for both locations to the extent that they are approximately co-trended (i.e., cointegrated). The log values of the time series for Cs-134 for Yokosuka NB plotted in Figure 3 may also be nonstationary. Further, as noted above, the Yokosuka NB time series is oppositely trended with time with a slope that is as positive as the slopes of the Yokota AB and IMS-Takasaki time series are negative.

The time structures of the time series of log values at Yokota AB, IMS-Takasaki, and Yokosuka NB were investigated using autocorrelation analysis. Autocorrelation (also referred to as serial correlation) is the cross-correlation of a time series with itself, that is, it is correlation between a variable lagged (that is, offset or shifted) one or more time periods and itself. The objective is to find temporal relationships, or their absence, between consecutive observations in these time series. In particular, autocorrelation is used for finding repeating patterns in the time series to detect non-randomness in the data. (Diebold, 2009; Bowerman and O'Connell, 1993; Madridakis et al., 1998; Hanke and Wichern, 2009; NIST/SEMATECH, 2015)

For a time series Y_t consisting of T consecutive (and equi-spaced) measurements, y_1, y_2, ..., y_T at times t_1, t_2, ..., t_T, the autocorrelation coefficient r_k at lag k is defined as:

$$r_k = \frac{\sum_{t=k+1}^{T} (y_t - \bar{y})(y_{t-k} - \bar{y})}{\sum_{t=1}^{T} (y_t - \bar{y})^2} \quad (1)$$

where $\bar{y}$ is the mean of all the data values in the time series. The autocorrelation coefficient r_k is a dimensionless statistic that measures the strength of the linear association between successive observations as a function of the time separation k between them. If the series is stationary the value of r_k should diminish rapidly towards zero as k increases. If the series is trended, r_k will decrease toward zero gradually with increasing lag. A k-period plot of autocorrelations is called an autocorrelation function (ACF).

Because the air activity concentration values of the time series range over several orders of magnitude, the many low values toward the end of the series are overwhelmed, i.e., "swamped," by the few large values early in the time series. The result is to effectively remove the autocorrelation in the data. To minimize this "swamping" effect of data ranging over several orders of magnitude, the (common) logarithms of the air activity concentrations were taken as before. ACFs were calculated according to equation (1) and plotted with the logarithmically-transformed data using Minitab®.

Figure 4 and Figure 5 display the ACF of the time series of log Cs-134 values for Yokota AB and IMS-Takasaki. The autocorrelations are shown as the blue vertical lines over their respective lag; the height of the line is the numerical value of the autocorrelation coefficient at that lag. The red dashed lines are the 5% significance limits for the autocorrelations. Autocorrelations above or below (for negative values) the dashed lines are statistically significant; autocorrelations within the dashed lines, as here, are not statistically significant. Note that for this ACF, the IMS-Takasaki time starts on March 15 (and not March 12 as for Yokota AB) because of the missing value for March 14. These figures are representative of the ACF results for the I-131 and Cs-137 time series at both Yokota AB and IMS-Takasaki shown in Appendix A-2.

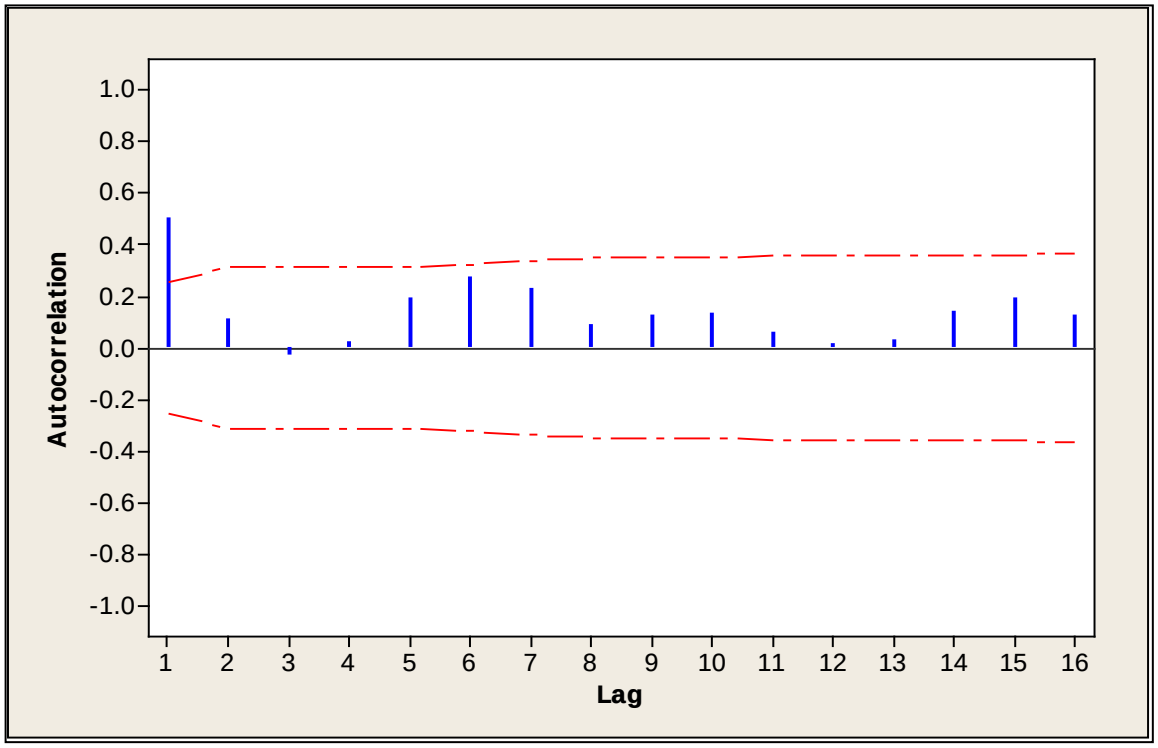

Figure 4. ACF of the logarithmic values of Cs-134 air activity concentration for Yokota AB

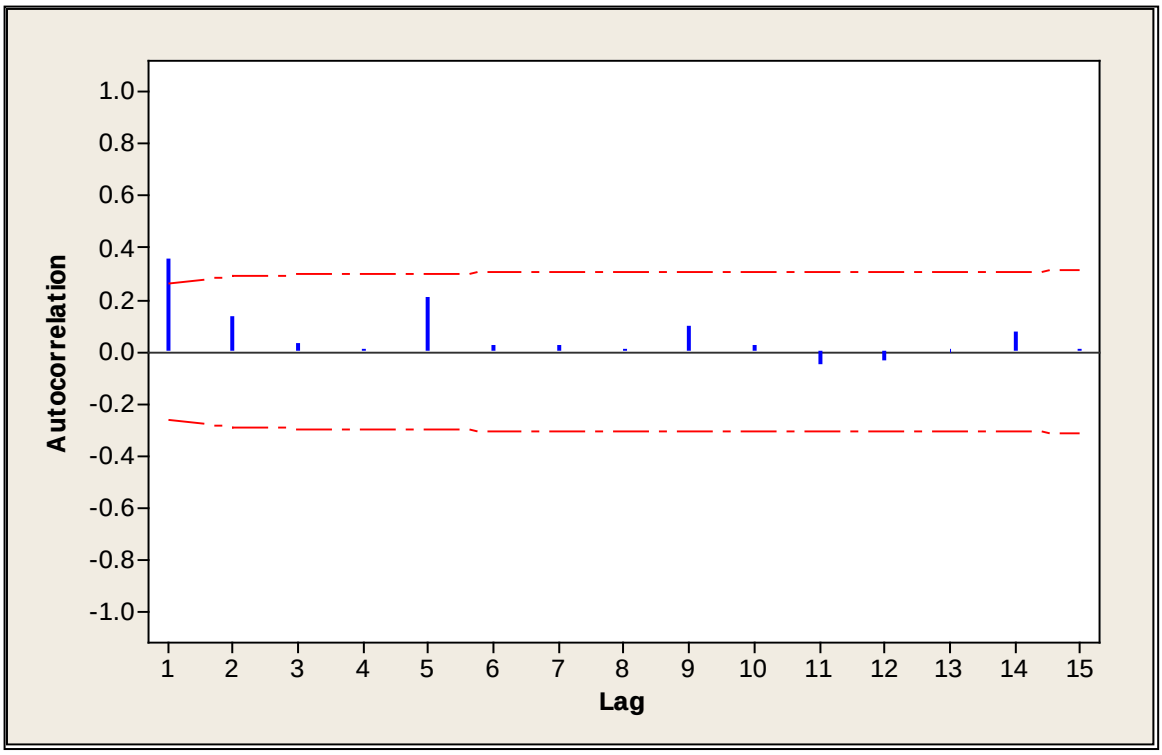

Figure 5. ACF of the logarithmic values Cs-134 air activity concentration for IMS-Takasaki

The autocorrelation coefficients of the log values of the time series at both locations show a decrease with increasing lag with a highly statistically significant leading coefficient r_1. This behavior is also seen for Cs-137 in Figure A-9 for IMS-Takasaki and Figure A-12 for Yokota AB. For I-131, the autocorrelation coefficients shown in Figure A-7 for IMS-Takasaki and Figure A-10 for Yokota AB display a gradual decrease with increasing lag with the first several coefficients being significant. For all radionuclides, this behavior is strong evidence indicating that the log values from both Yokota AB and IMS-Takasaki are nonstationary and trended (Diebold, 2009; Bowerman and O'Connell, 1993; Madridakis et al., 1998; Hanke and Wichern, 2009; NIST/SEMATECH, 2013). The ACF's reinforce the conclusion of trended nonstationarity already reached on the basis of the OLS time series regressions discussed above.

For the time series of Cs-134 log values for Yokosuka NB, the ACF was calculated for the data available from March 21 to April 11, deleting the days with missing observations (leaving a series of length $T = 15$). Collapsing the data in this fashion may risk altering the temporal structure that may be present in the data. An alternative was to fill the missing cases with calculated but inherently fictitious values, risking the same end; this latter approach was not pursued.

The ACF for the time series for Cs-134 log values for Yokosuka NB is shown in Figure 6 (the ACF of the log values of the time series for I-131 and Cs-137 from Yokosuka NB are generally similar as shown in Appendix A-2). None of the autocorrelation coefficients are statistically significant. This structure is most often encountered with stationary time series, more to the point, series that are not trended. Moreover, the algebraic signs of the autocorrelation

coefficients appear to alternate with increasing lag. Combining these observations, this pattern of alternating statistically insignificant coefficients is often seen for random data (e.g., white noise), which may likely be the case for the Yokosuka NB series.

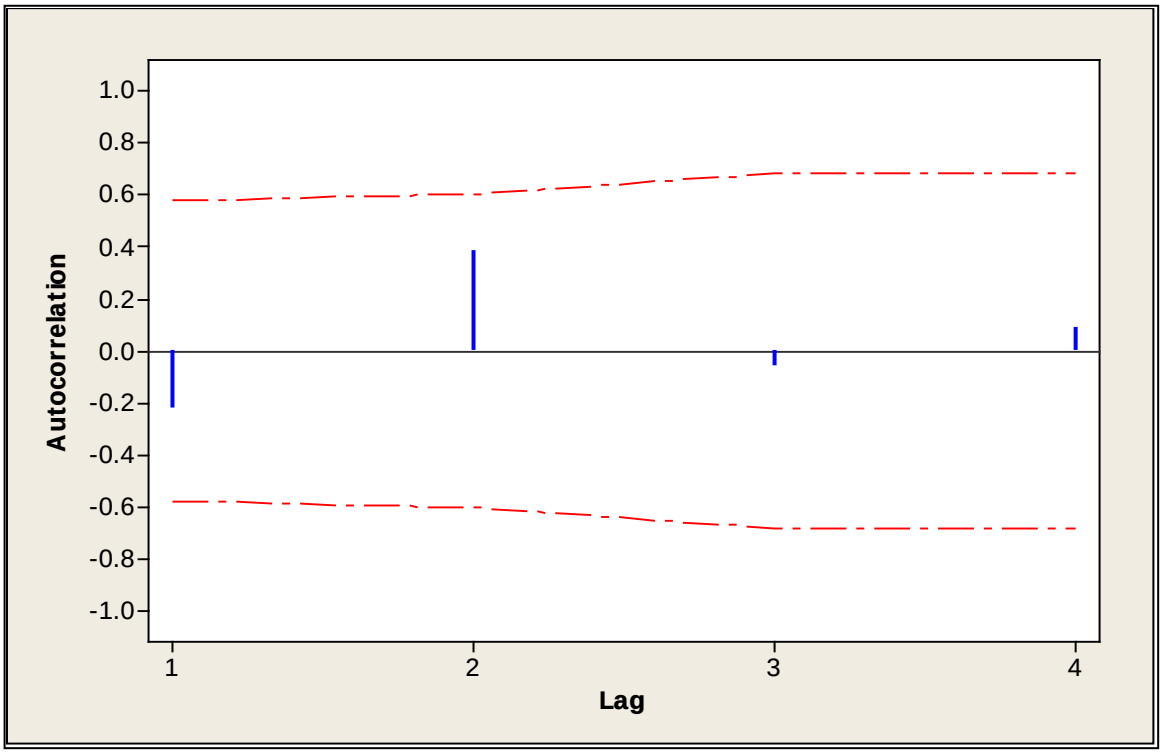

Figure 6. ACF of the logarithmic values of Cs-134 air activity concentration for Yokosuka NB

The above comparisons of Yokosuka NB to both Yokota AB and IMS-Takasaki for Cs-134 are also seen in the time series of logarithmic values of I-131 and Cs-137 air activity concentrations (Appendix A-2). The conclusion is that the logarithmically-transformed time series for Yokosuka NB does not exhibit the same temporal structure as does the corresponding time series from Yokota AB and IMS-Takasaki. Stated more specifically, the Yokosuka NB time series is distinctly different from those at the other two locations.

Transforming the data into changes ("deltas") rather than levels (actual values) can often eliminate the autocorrelation between observations in consecutive time periods. For a time series $Y = \{y_1, y_2, \ldots, y_T\}$, the changes are computed as "first differences" between consecutive observations:

$$\Delta y_t = y_t - y_{t\text{-}1} \tag{2}$$

for $t = 2, 3, \ldots, T$. If the resulting series of first differences is stationary, then it will appear essentially flat in a time series plot. Series whose nonstationarity is removed after first differencing are said to be integrated to first order, denoted by I(1). (Bowerman and O'Connell, 1993, Diebold, 2009; Hanke and Wichern, 2009; Madridakis et al., 1998; NIST/SEMATECH,

2015) Note that here the first differences represent daily differences in the log values of air activity concentration.

The first differences of the time series of log values for Yokota AB and IMS-Takasaki for Cs-134 were calculated according to equation (2) and are displayed in Figure 7. The first difference time series of log values for I-131 and Cs-137 at both locations very closely follow a similar pattern as those for Cs-134 (see Appendix A-3).

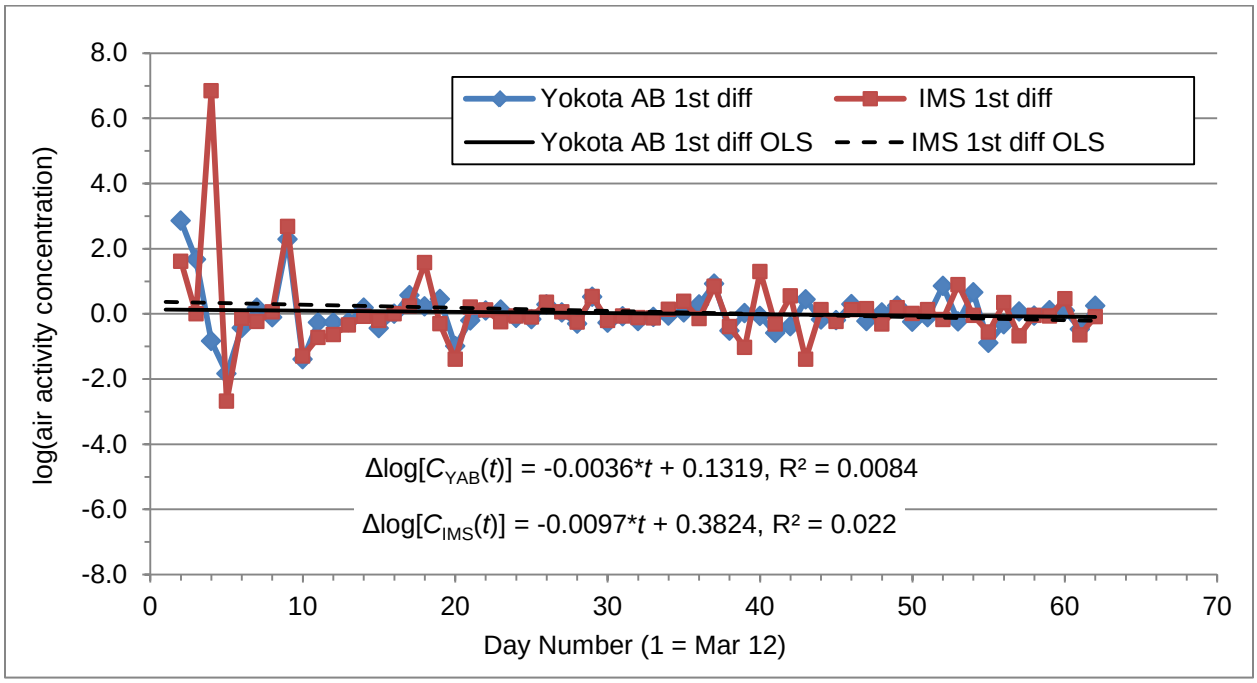

Figure 7. First differences in logarithmic values of air activity concentrations of Cs-134 for Yokota AB and IMS-Takasaki

The first differences of the time series of log values at both locations appear to fluctuate around the horizontal axis; after the first few days, the series settle down and appear relatively flat. Moreover, after the first few days, the values appear to be mostly constrained within a narrow band around the log (air activity concentration) line with a value of 0.0. That is, the deltas of the log values appear to be stationary in the long term. Consequently, the log values of the time series for both radionuclides at both locations appear to be I(1).

The first differences of the time series of log values for Cs-134 at Yokosuka NB were also calculated according to equation (2) and are displayed in Figure 8. Again, the first differences of the log values for I-131 and Cs-137 closely resemble those for Cs-134 (see Appendix A-3). Note that the first differences of the log values of the time series for both radionuclides at Yokosuka NB do not seem to fluctuate around the horizontal axis. Instead, the deltas appear to increase with time. An OLS regression to the first differences in the log values at Yokosuka NB (Figure 8) show that they are positively trended. Also, the scatter appears to wander considerably and chaotically. It cannot be concluded that the first differences of the log values for Cs-134 at Yokosuka NB is stationary and hence it cannot be concluded to be I(1). Likewise, it cannot be concluded that the first differences time series of log values for I-131 and

Cs-137 from Yokosuka NB are I(1). However, these conclusions may be equivocal given the short series length of the Yokosuka NB series.

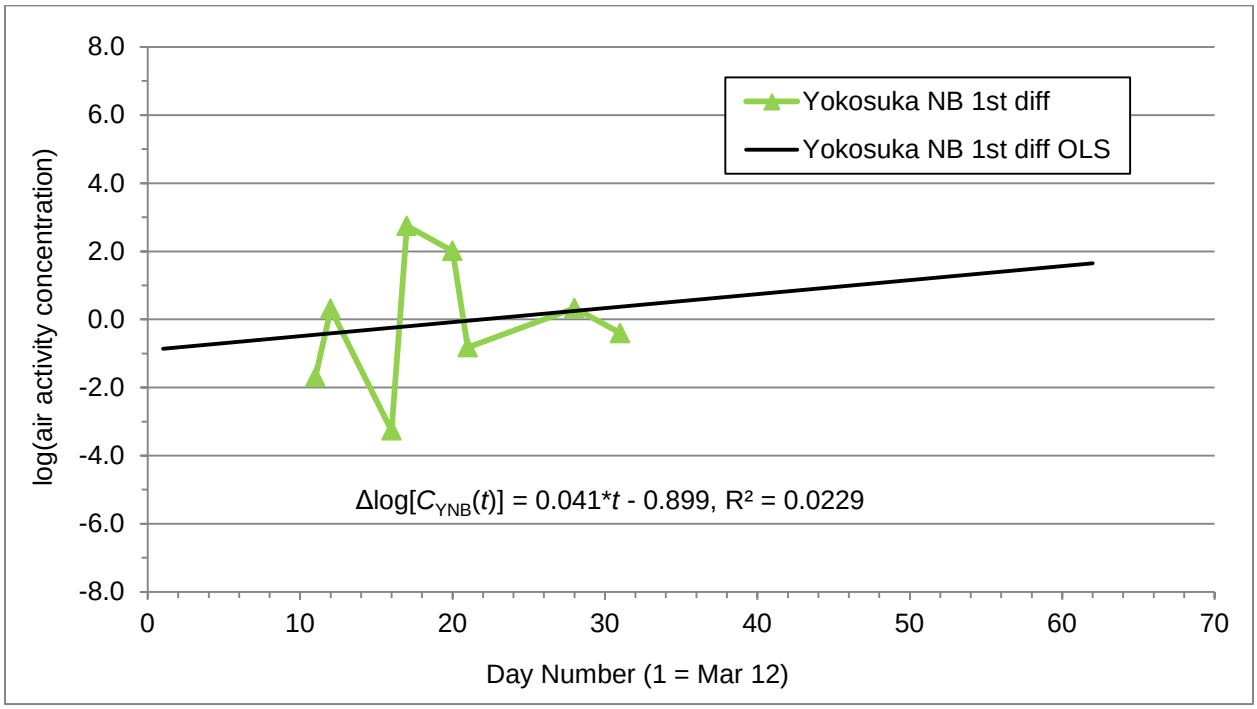

Figure 8. First differences in logarithmic values of Cs-134 air activity concentration at Yokosuka NB from March 21 to April 11

3.2 Time Series Cointegration

Here, the econometric concept of cointegration is applied to the diagnostic checking of the log values of the time series of air activity concentration. Consider two time series $X(t)$ and $Y(t)$. There are two distinct possibilities: Either the two series drift apart over time or the two series move in tandem, not departing too much from each other. In the latter case, the series have common or shared trends and are said to be co-trended or "cointegrated." Cointegrated time series possess a long-run steady state toward which the series converge. While in any individual time period there may be short run deviations from the long term steady state, these deviations are offset by oppositely directed deviations in later periods with the cumulative effect that the series stay co-trended with one another (Granger, 1981; Engle and Granger, 1987; Murray, 2006; Nachane, 2006; Tong et al., 2011). The task here is to determine whether or not the time series of log values of air activity concentration are cointegrated. Note that as used here cointegration does not imply causality, i.e., one time series does not cause the other to move as it does. Rather it is the physics of radioactive decay and of atmospheric transport and dispersion as well as the commonality of the terrain and meteorology that cause the series to move together.

The first step in testing for cointegration is to estimate the "cointegration" OLS equations of the form:

$$Y(t) = \varphi + \theta X(t) + u(t) \tag{3}$$

where φ and θ are constants and $u(t)$ denotes the residuals from the regression. For each radionuclide (Cs-134, Cs-137, and I-131), the following pairwise bivariate cointegrating OLS regressions of the time series of log values of air activity concentration were performed:

$$\log[C_{YAB}(t)] = \varphi_1 + \theta_1 \log[C_{IMS}(t)] + u_1(t) \tag{4a}$$

$$\log[C_{YNB}(t)] = \varphi_2 + \theta_2 \log[C_{YAB}(t)] + u_2(t) \tag{4b}$$

$$\log[C_{YNB}(t)] = \varphi_3 + \theta_3 \log[C_{IMS}(t)] + u_3(t) \tag{4c}$$

Figure 9 displays the series $\log[C_{YAB}(t)]$ vs. $\log[C_{IMS}(t)]$ for Cs-134. An OLS regression for equation (4a) was performed; the resulting cointegrating equation and its R^2 value are also displayed in Figure 9 (the cointegration equation is plotted over the data). This figure is representative of the results for Cs-137 and I-131 shown in Appendix A-4. In particular, the cointegrating equation is positively correlated with a fairly high R^2 value. The coefficient of.

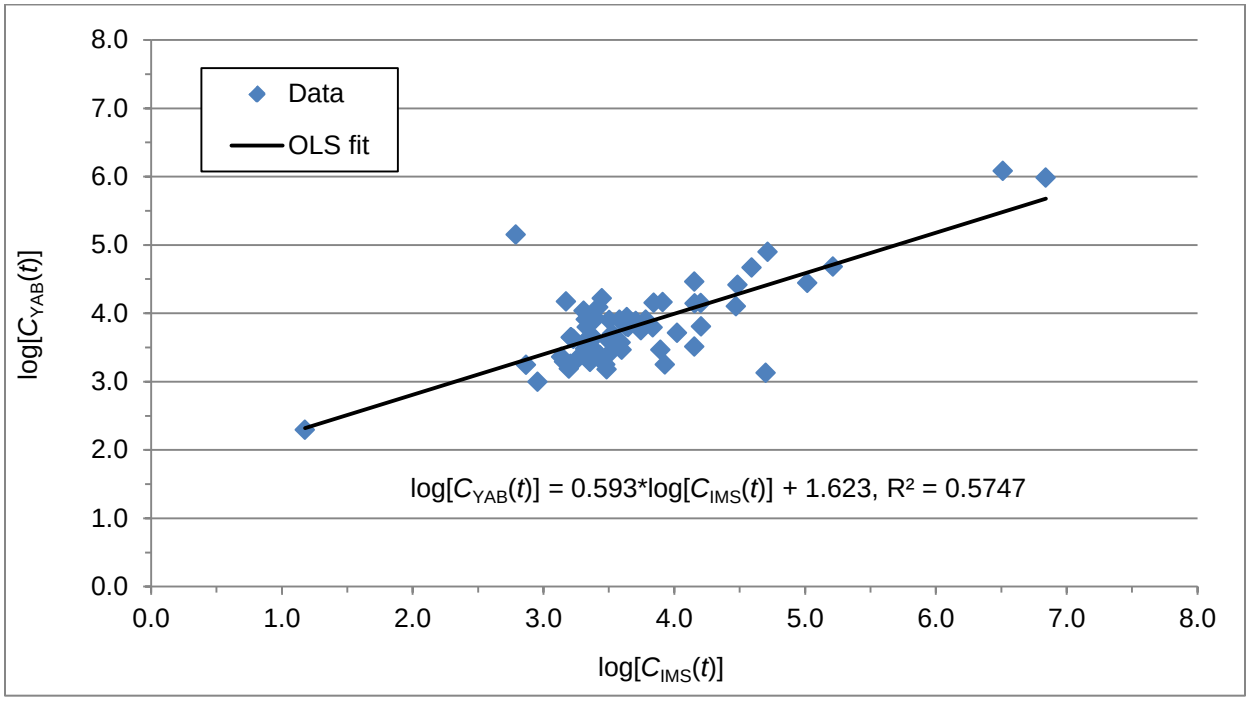

Figure 9. Cointegrating OLS relationship between Yokota AB and IMS-Takasaki for Cs-134

determination R^2 is over 0.5 and means that more than half of the variation in $\log[C_{YAB}(t)]$ is accounted for by varying $\log[C_{IMS}(t)]$ according to the OLS regression equation. Note that for

these regressions, $T = 61$. The cointegrating equations between the time series of log values at Yokota AB and IMS-Takasaki for each of the three radionuclides are highly statistically significant on the basis of the test statistics (t and p values) of the coefficient on $\log[C_{IMS}(t)]$ in the OLS fit. Furthermore, the data points appear to be fairly well clustered around the cointegration equation, again indicating a good fit

The situation is different comparing the time series of log values for Yokosuka NB to those for Yokota AB and to those for IMS-Takasaki. The results for Cs-134 are as shown in Figure 10 and Figure 11. Also displayed on these figures are the results of OLS regressions for the cointegrating equations (4b) and (4c) and their R^2 values, respectively (the cointegration equations are the black lines plotted over the data). The results for Cs-137 and for I-131 are fairly similar to those for Cs-134 (see Appendix A-4).

The OLS regressions shown in Figure 10 and Figure 11 are weak relationships (on the basis of the low values of R^2). Furthermore, the data points in both these graphs appear to be widely scattered about the cointegration equation, indicating poor fits. More importantly and more obviously, these cointegrating equations are negatively correlated. As such, they are all oppositely directed to the corresponding $\log[C_{YAB}(t)]$ vs. $\log[C_{IMS}(t)]$ cointegrating equation shown in Figure 9. There, high values at one location are associated with high values at the other. Here, high values at Yokosuka NB are associated with low values at the other locations and vice versa, which is counterintuitive. In addition, the cointegrating equations of the time series of log values between Yokosuka NB and either Yokota AB or IMS-Takasaki for each of the three radionuclides are not statistically significant on the basis of the test statistics (t and p values) of the coefficients on $\log[C_{YAB}(t)]$ and $\log[C_{IMS}(t)]$ in the OLS fits displayed in these figures. These

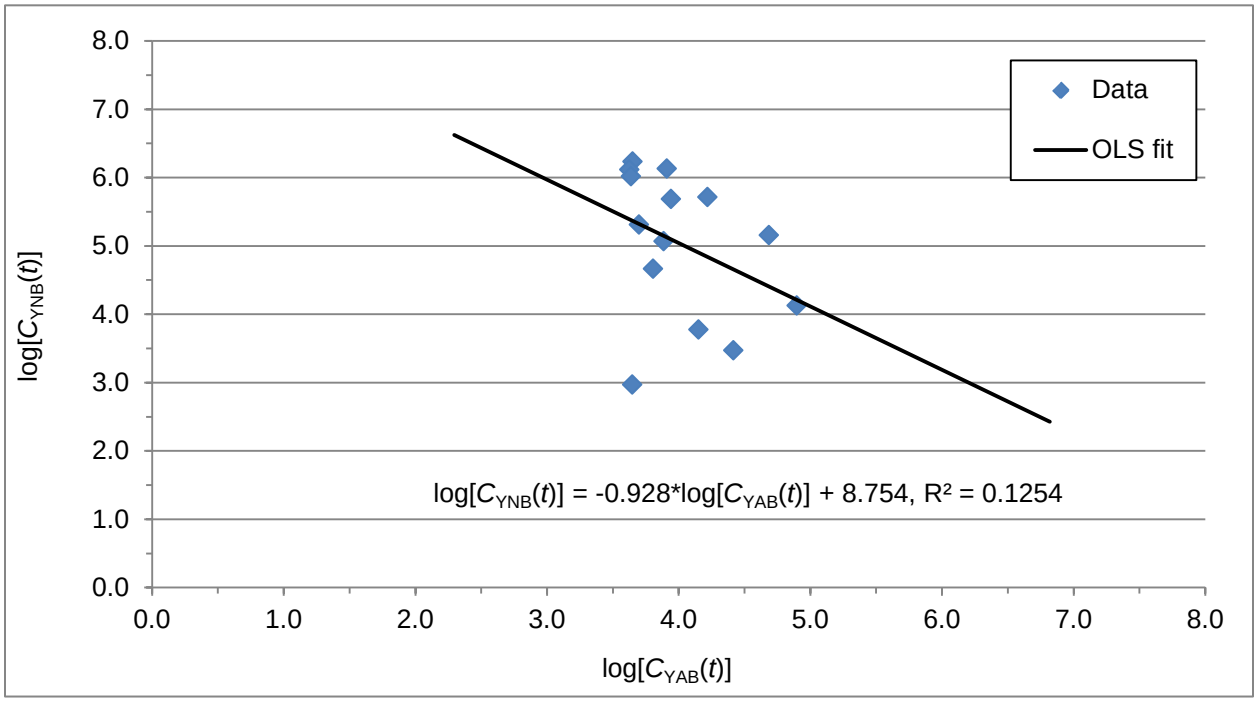

Figure 10. Cointegrating OLS relationship between Yokosuka NB and Yokota AB for Cs-134

behaviors are representative of the cointegrating equations determined for Yokosuka NB to those for Yokota AB and to those for IMS-Takasaki for both Cs-137 and I-131.

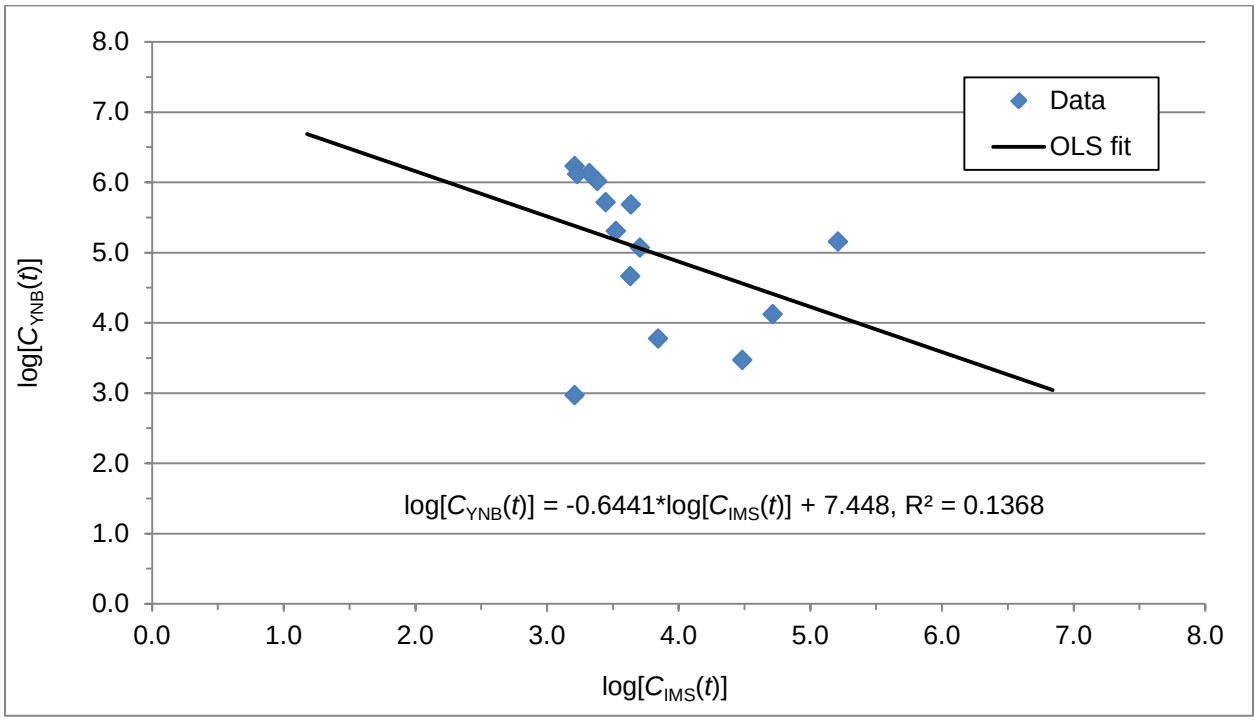

Figure 11. Cointegrating OLS relationship between Yokosuka NB and IMS-Takasaki for Cs-134

It was shown in Section 3.1 that the Yokota AB and IMS-Takasaki time series for all three radionuclides are I(1) in that their nonstationarity is removed by first differencing ("deltas"). It was also suggested that the Yokosuka NB time series may not be I(1). For the discussion here, it will be temporarily assumed that the Yokosuka NB time series for all three radionuclides are also I(1).

For two time series x_t and y_t which are both I(1), there exists a linear combination:

$$\alpha x_t + \beta y_t = \varepsilon_t \tag{5}$$

where α and β are constants and ε_t is a stationary white noise series with zero mean and constant variance. This is called the cointegration theorem. The ordered pair (α, β) is called the cointegrating vector. In so doing, this linear combination eliminates the common trends shared by x_t and y_t and produces a white noise series. Conversely, if such a vector can be found, then the time series are cointegrated. (Granger, 1981; Engle and Granger, 1987; Murray, 2006; Nachane, 2006; Tong et al., 2011)

Here, one series is subtracted from another and the result is examined for stationarity; if the series difference is stationary then the series are cointegrated with the cointegrating vector (1, −1). For each of the three radionuclides, the following differences are calculated: (1) $\log[C_{YAB}(t)] - \log[C_{IMS}(t)]$, (2) $\log[C_{YNB}(t)] - \log([C_{YAB}(t)]$, and (3) $\log[C_{YNB}(t)] -$

log[$C_{IMS}(t)$]. If any of these series differences produces a stationary series ε_t, then the pair of series that were differenced is cointegrated. The results for Cs-134 are displayed in Figure 12. Similar results are obtained for I-131 and Cs-137 (see Appendix A-5).

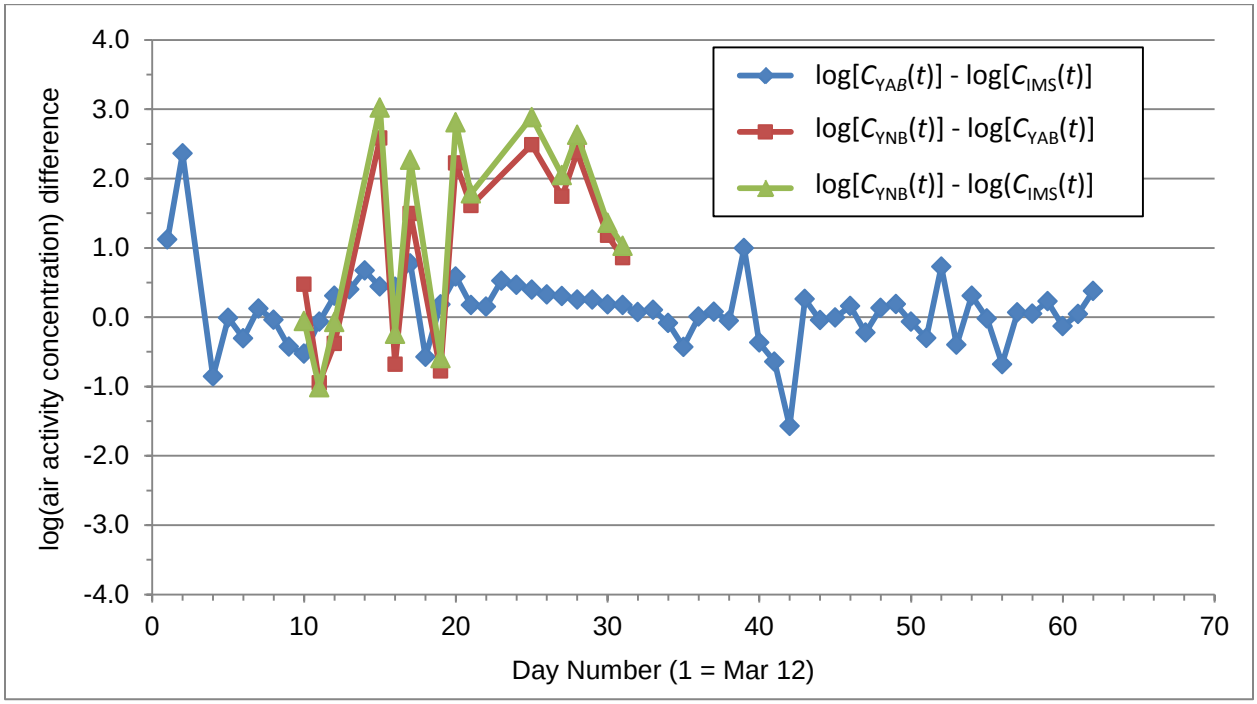

Figure 12. Pairwise differences of the logarithmic values of air activity concentration for Cs-134 for the three locations

The blue curve is the difference log[$C_{YAB}(t)$] − log[$C_{IMS}(t)$]. Note that after a short initial period of two or three days, this curve seems to stabilize about the horizontal axis and so appears to essentially have a zero mean, a requirement for the stationarity of the error series ε_t. Moreover, the fluctuations about the mean appear to be confined within a narrow band around the horizontal axis, evidence that the variance is finite and approximately constant, a further requirement for the stationarity of the ε_t. Hence, this difference series appears to be random, e.g., "white noise." In the ACF of this differenced series (not shown), the autocorrelation coefficients are all statistically insignificant and alternate in their algebraic signs with increasing time lag, again indicating that this is a white noise series.

As a result, in equation (5), $\alpha = 1$ and $\beta = -1$. Therefore, it may be concluded that the series log[$C_{YAB}(t)$] and log[$C_{IMS}(t)$] are, indeed, cointegrated with cointegrating vector (1, −1). More to the point, log[$C_{YAB}(t)$] and log[$C_{IMS}(t)$] are co-trended with each other.

The situation is dramatically different for the series resulting from differencing from log[$C_{YNB}(t)$], specifically, log[$C_{YNB}(t)$] − log[$C_{YAB}(t)$] and log[$C_{YNB}(t)$] − log[$C_{IMS}(t)$]. The series oscillate widely around the horizontal with a nonzero mean. Moreover, the variance is obviously non-constant. As a result, it may be concluded that for all three radionuclides, differencing from log[$C_{YNB}(t)$] does not produce a stationary (white noise) series. Indeed, all linear combinations according to equation (5) that were attempted failed to produce a white noise

series. It may be concluded that $\log[C_{YNB}(t)]$ is not cointegrated with either $\log[C_{YAB}(t)]$ or with $\log[C_{IMS}(t)]$, i.e., $\log[C_{YNB}(t)]$ does not share a common trend with either $\log[C_{YAB}(t)]$ or with $\log[C_{IMS}(t)]$.

3.3 Summary and Discussion

The results presented herein show that time series for the time series of log values of air activity concentration from IMS-Takasaki and Yokota AB are consistent with each other. Autocorrelation analysis shows the time series from these locations are trended and that their trends share similar time structure. The trends of these times series could be removed by first differencing, an important property for cointegration. Cointegration showed that these time series share similar trends in time and appear to move together towards a long-term steady value.

The results also show that the time series of log values for Yokosuka NB are quantitatively inconsistent and incompatible with the corresponding log values of the time series from both Yokota AB and IMS Takasaki. Indeed, for all three radionuclides, the logarithmic Yokosuka NB series are fundamentally and inherently different from their Yokota AB and IMS-Takasaki counterparts. The time series of log values at Yokosuka NB do not have the time structure shared by the series at the other two locations. The nonstationarity of these series from Yokosuka NB could not be conclusively removed by first differencing. Finally, and perhaps most compelling, the logarithmic Yokosuka NB series could not be cointegrated with their counterparts at the other two locations. On this basis, the time series of log values at Yokosuka NB could not be shown to share a common time trend with the corresponding series from Yokota AB and IMS-Takasaki. The caveat is the limited number of values in the time series for Yokosuka NB which were used to arrive at these results.

These observations for the logarithmic values also apply to the original data. Therefore, the time series for Yokosuka NB for air activity concentration are quantitatively different from the corresponding time series from either Yokota AB or IMS-Takasaki, which are similar to each other. More specifically, this analysis demonstrates the inconsistent nature of the time series from Yokosuka NB as opposed to those from either Yokota AB or IMS-Takasaki. Furthermore, the analysis reported here lends some statistical support to the decision stated in Cassata et al. (2012) to reject the Yokosuka NB data as unusable for dose assessments and to replace it with the corresponding time series for Yokota AB.

This study further highlights the problematic nature of arbitrary selection of some data points from within a larger set of data. This leads to the recognition of the benefits of continuous (or frequent) sampling as opposed to sampling at arbitrary time intervals. This also points to the problematic nature of arbitrary selection of some data points from a larger set of data.

Section 4.

Conclusions

The econometric methods of autocorrelation analysis and cointegration were applied successfully to the analysis and comparison of time series of air activity concentrations of three radionuclides at Yokota AB, IMS-Takasaki, and Yokosuka NB in the Kanto Plain Region of Japan.

The results of autocorrelation analysis and cointegration analysis demonstrate that the time series of log values of air activity concentrations from IMS-Takasaki and Yokota AB are consistent with each other because they share similar trends in time structure and can be cointegrated. Conversely, the results indicate that the log values of the time series of air activity concentrations for Yokosuka NB do not exhibit the temporal structure of the corresponding time series from both Yokota AB and IMS-Takasaki. Indeed, the time series of log values from Yokosuka NB are inconsistent with and are distinctly different from their counterparts from the other two locations.

This econometric analysis reinforces a conclusion stated in Cassata et al. (2012) that the air sampling data for Yokosuka Naval Base are deemed less reliable than the Yokota Air Base data for southern Kanto Plain military bases.

The successful application of the econometric methods that were presented in the cases discussed herein suggest they may be valuable in other radiation dose assessments that are based, in part, on time series of measured radiological quantities.

Section 5.

References

Bowerman, B.L. and O'Connell, B.L., 1993. *Forecasting and Time Series: An Applied Approach*, 3rd Edition, Duxbury, Pacific Grove, CA.

Cassata, J., Falo, G., Rademacher, S., Alleman, L., Rosser, C., Dunavant, J., Case, D., and Blake, P., 2012. *Radiation Dose Assessments for Shore-Based Individuals in Operation Tomodachi, Revision 1*. DTRA-TR-12-001 (R1), Defense Threat Reduction Agency, Fort Belvoir, VA. December 31.

Chehata M., Dunavant J., Mason C., McKenzie-Carter M., Singer, H., 2013. *Probabilistic Analysis of Radiation Doses for Shore-Based Individuals in Operation Tomodachi*. DTRA-TR-12-002, Defense Threat Reduction Agency, Fort Belvoir, VA. May 21.

Diebold, F.X., 2009. *Elements of Forecasting, 4th Edition*, Cengage, Mason, OH.

Engle, R.F. and Granger, C.W.J., 1987. "Co-Integration and Error Correction: Representation, Estimation, and Testing," *Econometrica, 55*(2), 251-276.

Granger, C.W.J., 1981. "Some Properties of Time Series Data and Their Use in Econometric Model Specification," *J. Econometrics, 16*, 121-130.

Hanke, J.E. and Wichern, D.W., 2009. *Business Forecasting, 9th Edition*, Pearson Prentice Hall, Upper Saddle River, NJ.

Madridakis, S., Wheelwright, S.C., and Hyndman, R.J., 1998. *Forecasting: Methods and Applications, 3rd Edition*, John Wiley & Sons, NY.

Marro, R., McKenzie-Carter, M., Rademacher, S., Knappmiller, K., Ranellone, R., Case, D., Dunavant, J., and Miles, T., 2014. *Radiation Dose Assessments for Fleet-Based Individuals in Operation Tomodachi, Revision 1*. DTRA-TR-12-041 (R1), Defense Threat Reduction Agency, Fort Belvoir, VA. April 30.

Murray, M.P., 2006. *Econometrics: A Modern Introduction*, Pearson Addison Wesley, Boston, MA.

Nachane, D.M., 2006. *Econometrics: Theoretical Foundations and Empirical Perspectives*, Oxford University Press, New Delhi, India.

NIST (National Institute of Standards and Technology), 2015. *NIST/SEMATECH e-Handbook of Statistical Methods*. (http://www.itl.nist.gov/div898/handbook/, accessed April, 2015).

Rademacher, S.E., 2013. Email from Steven Rademacher, Chief, Radioactive Materials Licensing and Safety, HQ Air Force Safety Center, to Mondher Chehata, SAIC, "Subject: Dr. Singer's Statistical Comparison Report," August 22.

Tong, H., Kumar, T.K., and Huang, Y., 2011. *Developing Econometrics*, John Wiley & Sons, New York, NY.

Appendix A.

Plots of Air Concentration Data and Statistical Analysis Results

This appendix contains plots of the time series of activity concentrations, autocorrelation functions, first differences, cointegration, and pairwise comparisons of I-131, Cs-134 and Cs-137 at IMS-Takasaki, Yokota Air Base (AB), and Yokosuka Naval Base (NB) for the time period March 12 through May 12, 2011.

A-1. Time Series

A-1.1. Iodine-131

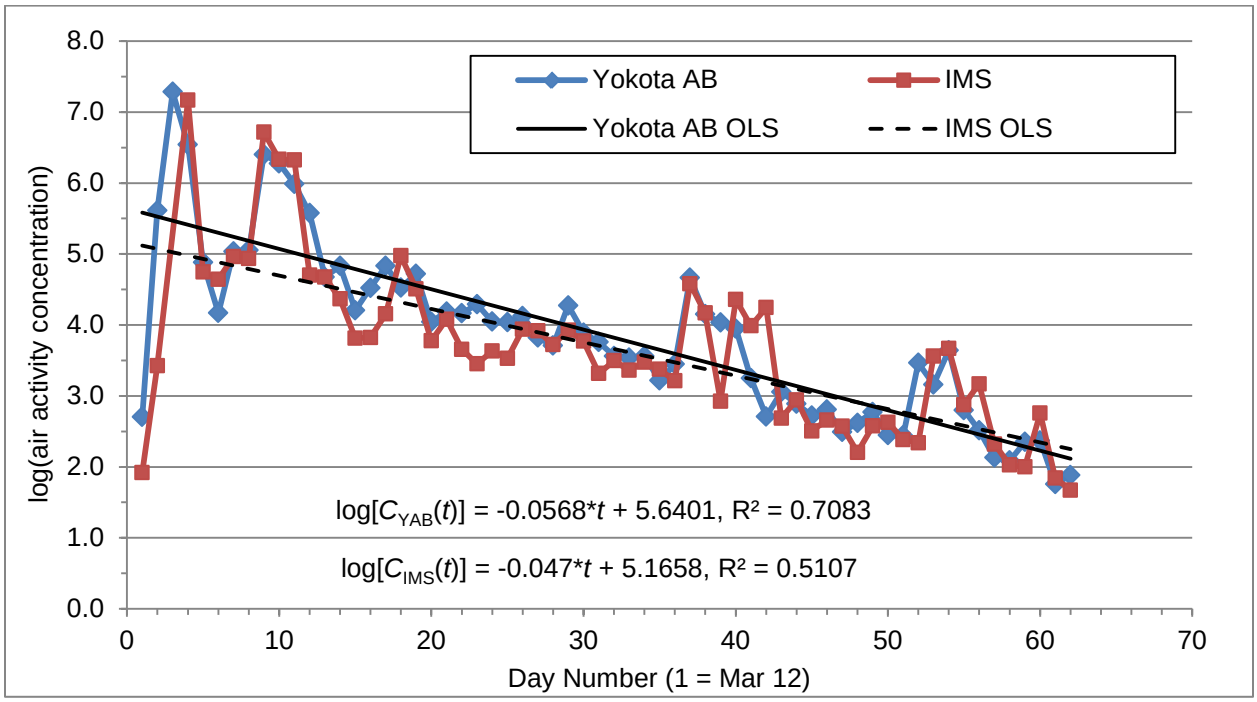

Figure A-1. Logarithmic values of I-131 air activity concentration for Yokota AB and IMS-Takasaki

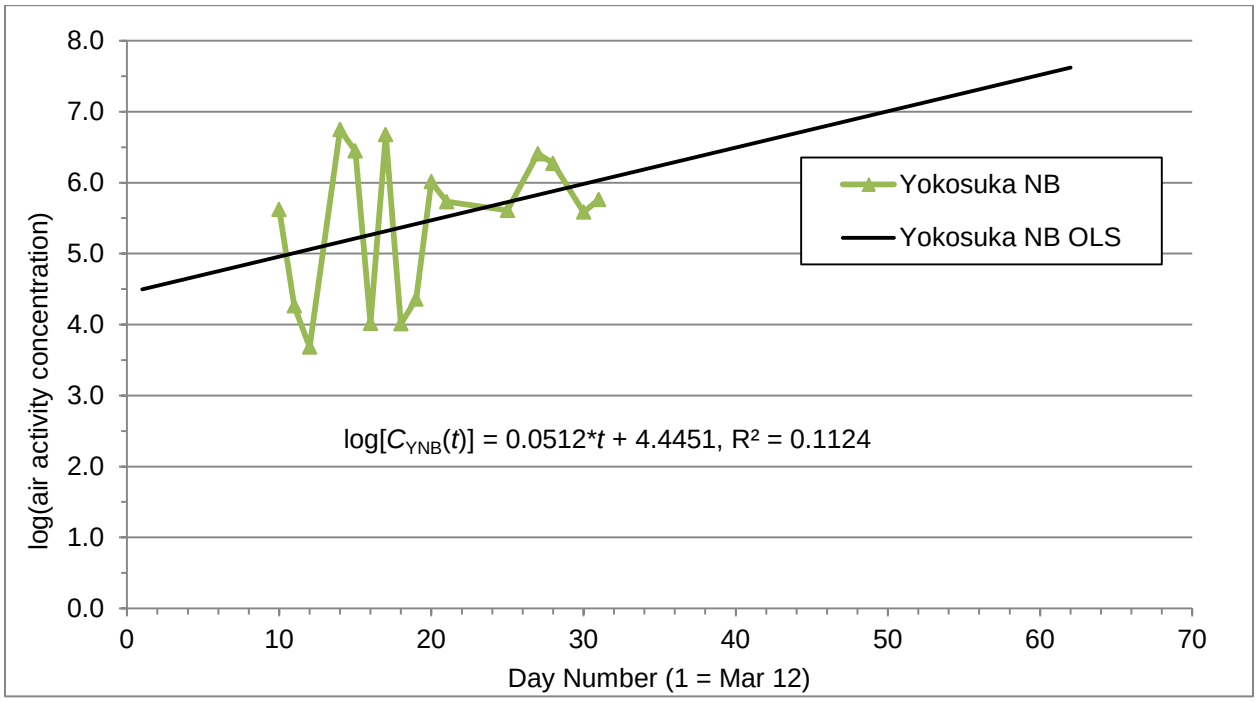

Figure A-2. Logarithmic values of I-131 air activity concentration for Yokosuka NB

A-1.2. Cesium-134

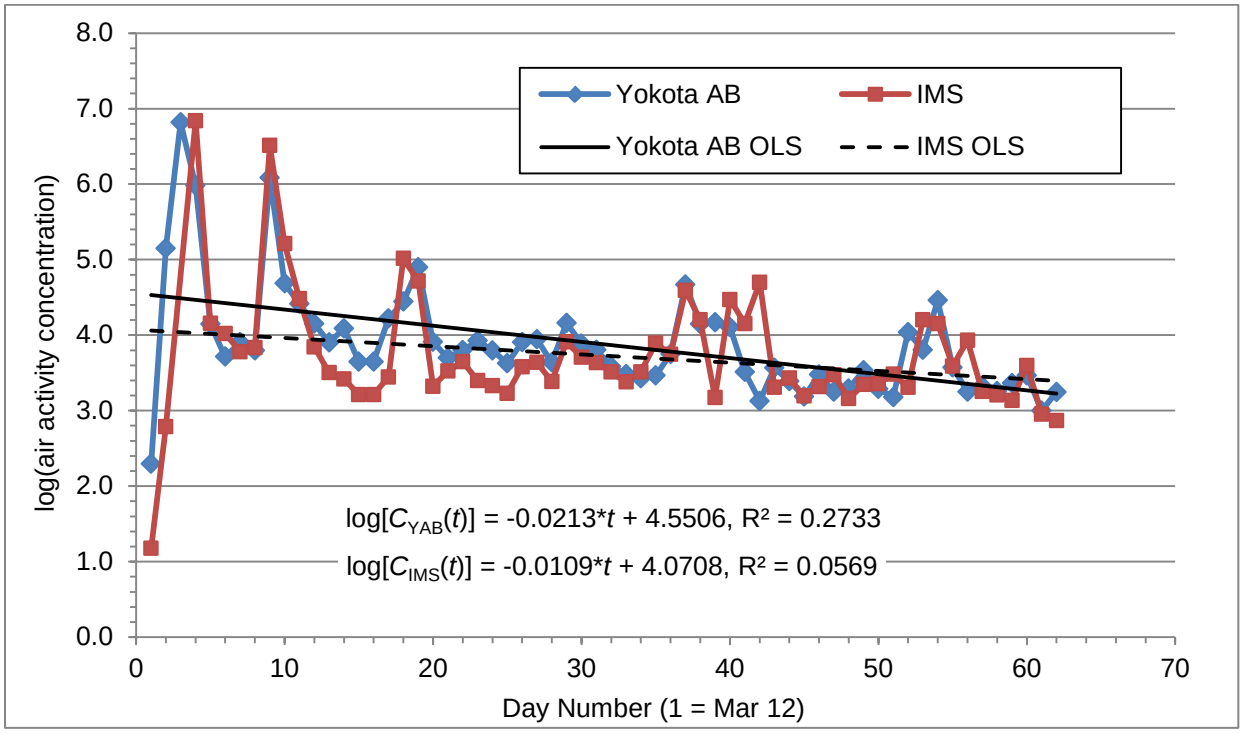

Figure A-3. Logarithmic values of Cs-134 air activity concentration for Yokota AB and IMS-Takasaki

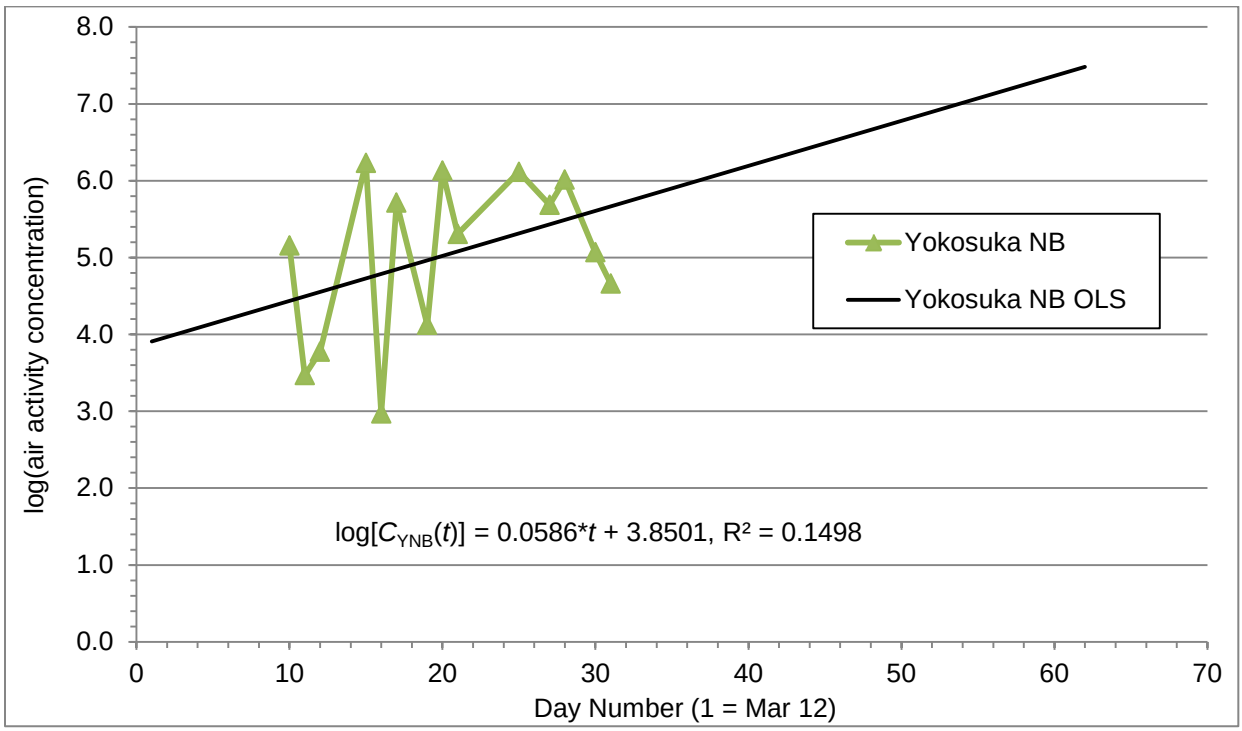

Figure A-4. Logarithmic values of Cs-134 air activity concentration for Yokosuka NB

A-1.3. Cesium-137

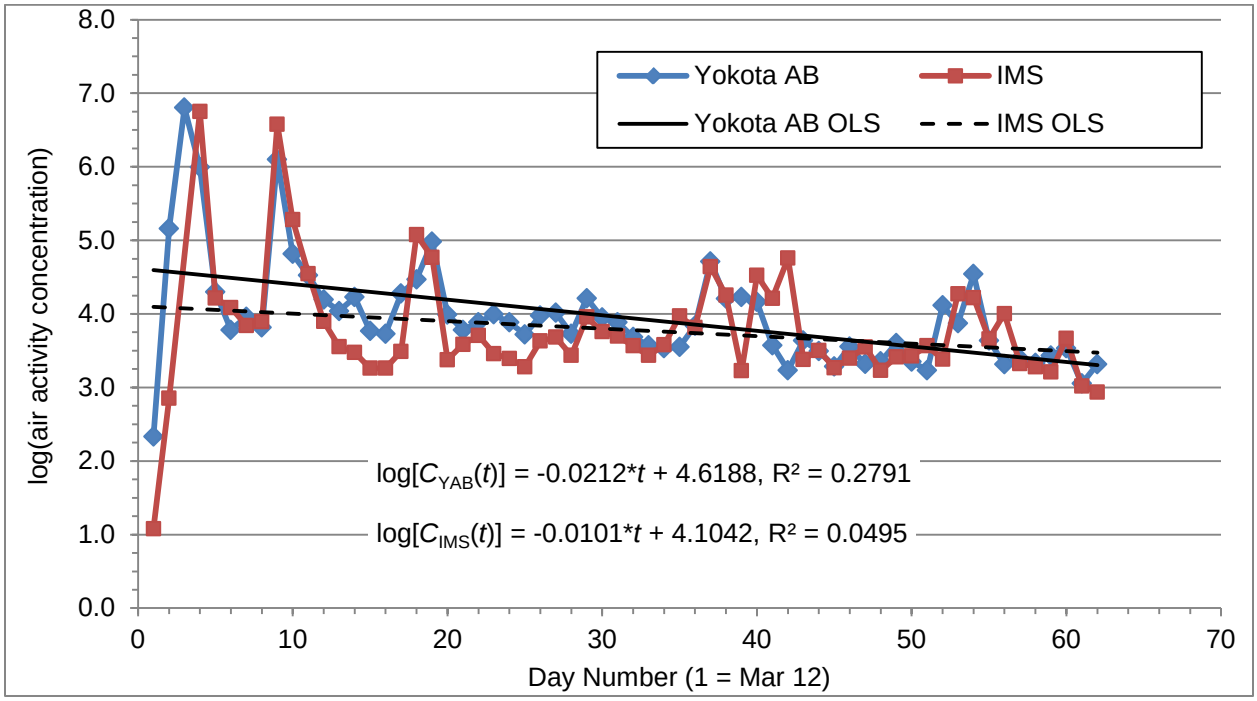

Figure A-5. Logarithmic values of Cs-137 air activity concentration for Yokota AB and IMS-Takasaki

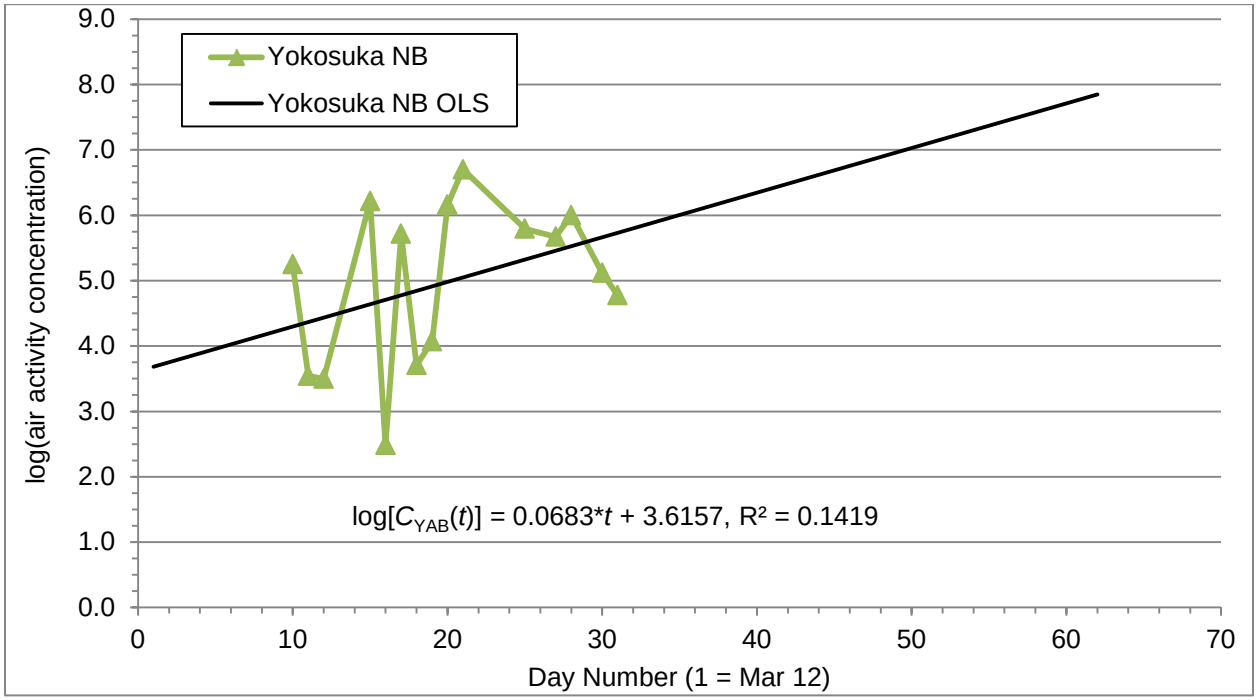

Figure A-6. Logarithmic values of Cs-137 air activity concentration for Yokosuka NB

A-2. Autocorrelation Functions

A-2.1. IMS-Takasaki

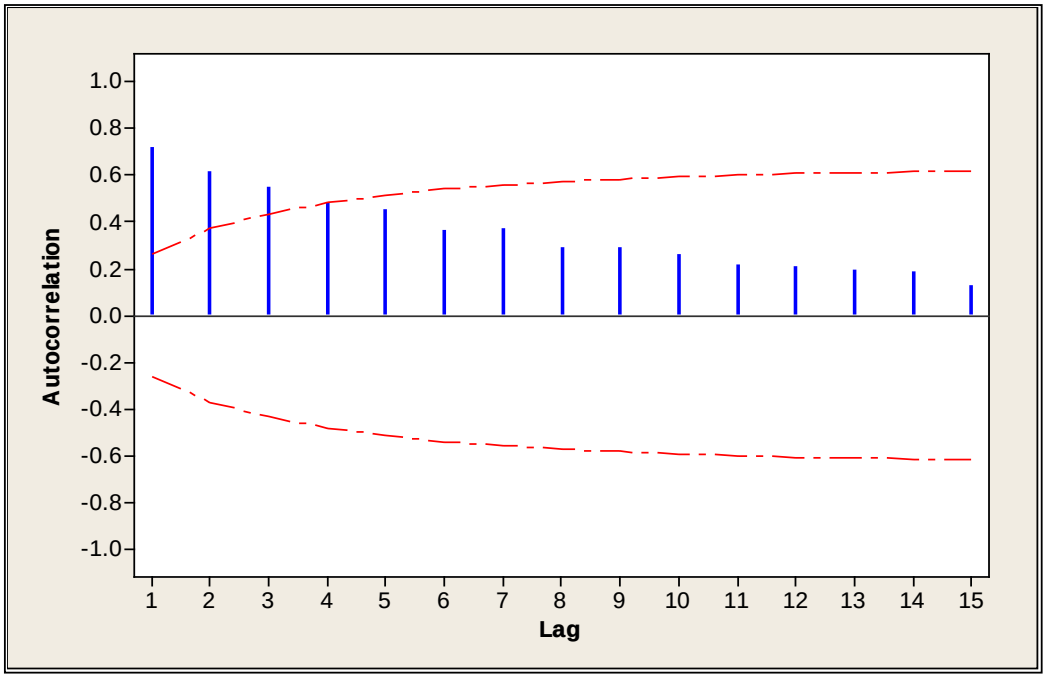

Figure A-7. ACF of the logarithmic values of I-131 air activity concentration for IMS-Takasaki

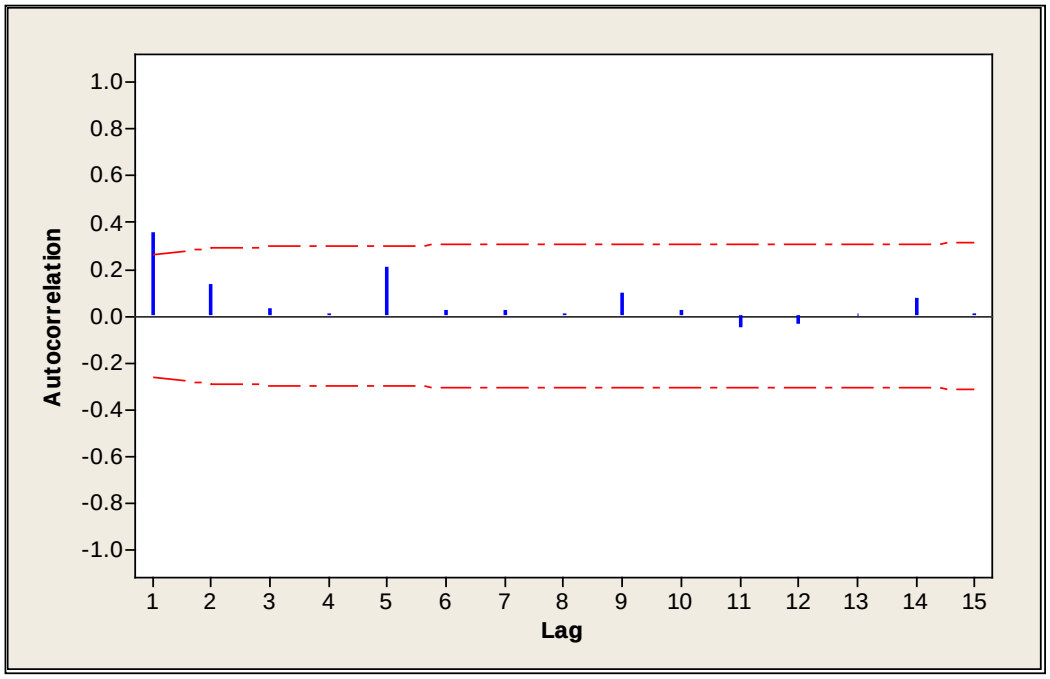

Figure A-8. ACF of the logarithmic values of Cs-134 air activity concentration for IMS-Takasaki

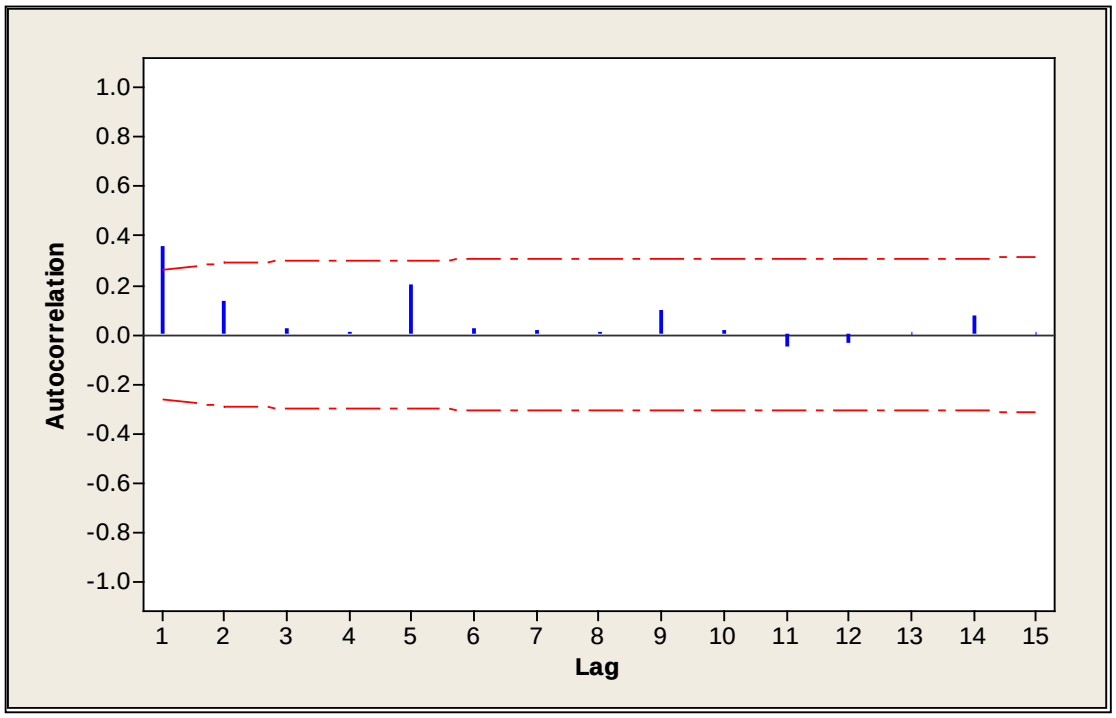

Figure A-9. ACF of the logarithmic values of Cs-137 air activity concentration for IMS-Takasaki

A-2.2. Yokota Air Base

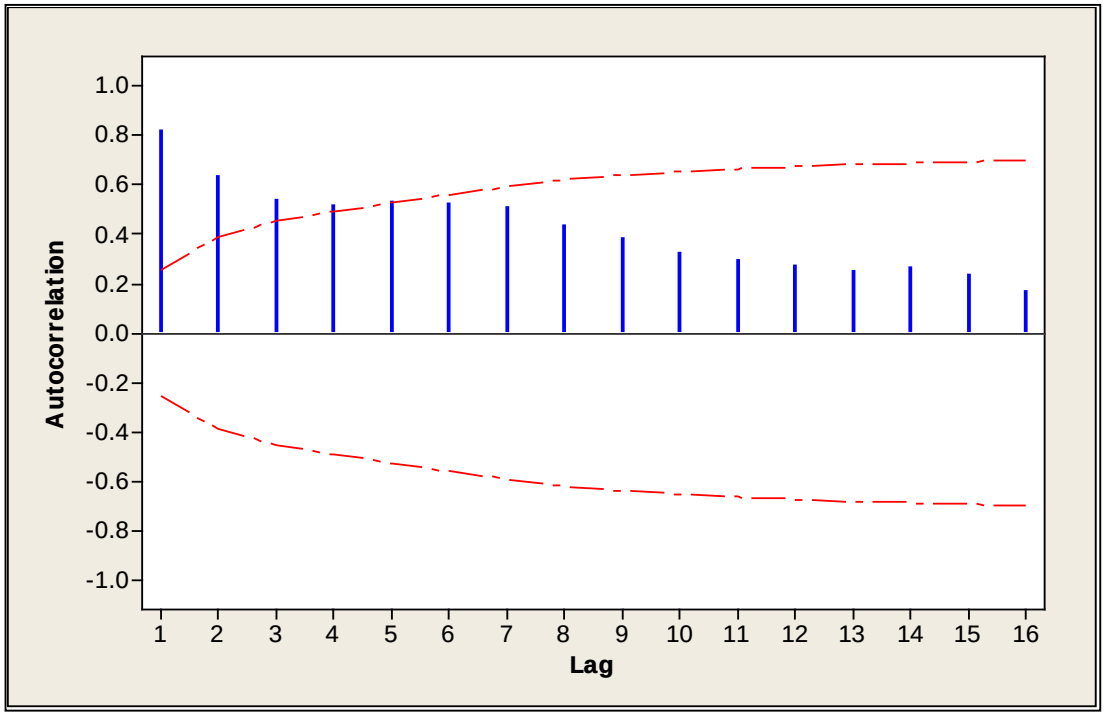

Figure A-10. ACF of the logarithmic values of I-131 air activity concentration for Yokota AB

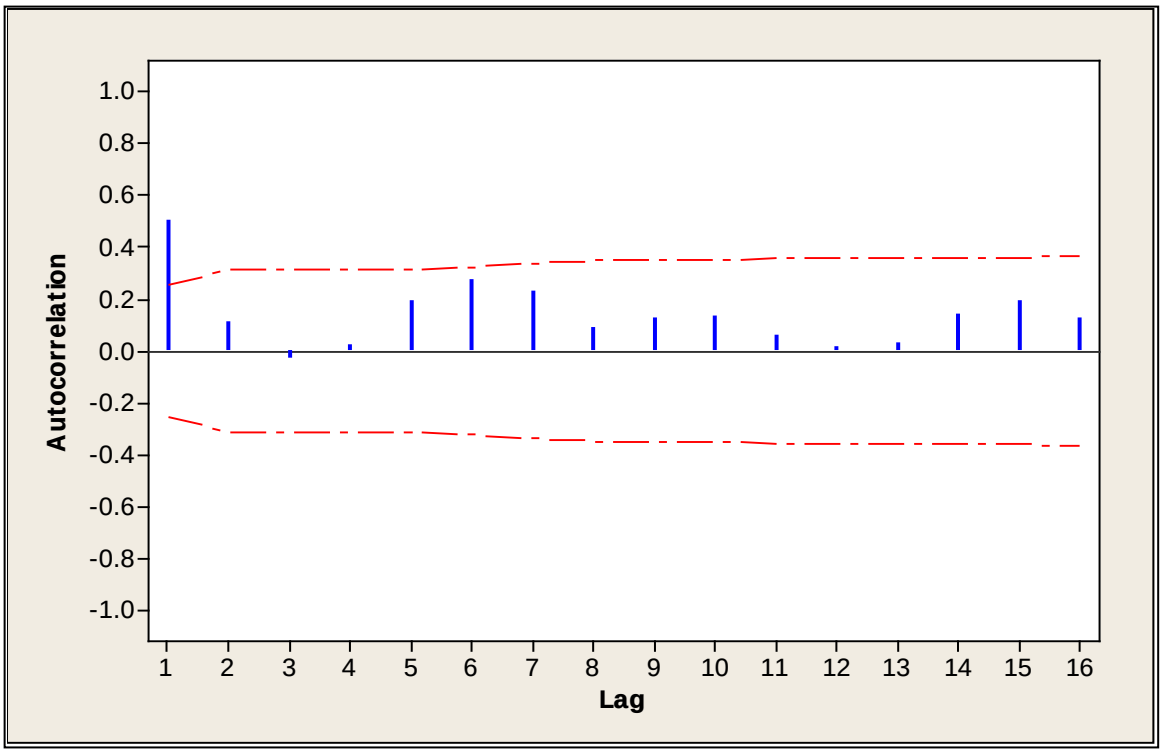

Figure A-11. ACF of the logarithmic values of Cs-134 air activity concentration for Yokota AB

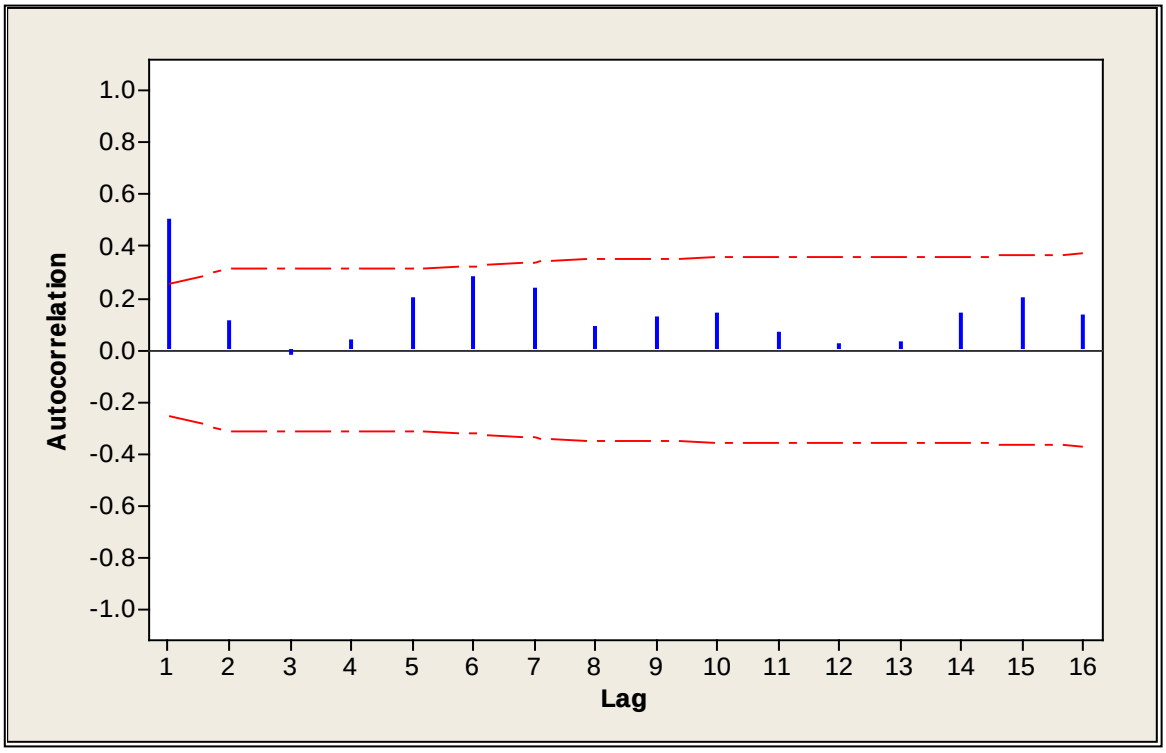

Figure A-12. ACF of the logarithmic values of Cs-137 air activity concentration for Yokota AB

A-2.3. Yokosuka Naval Base

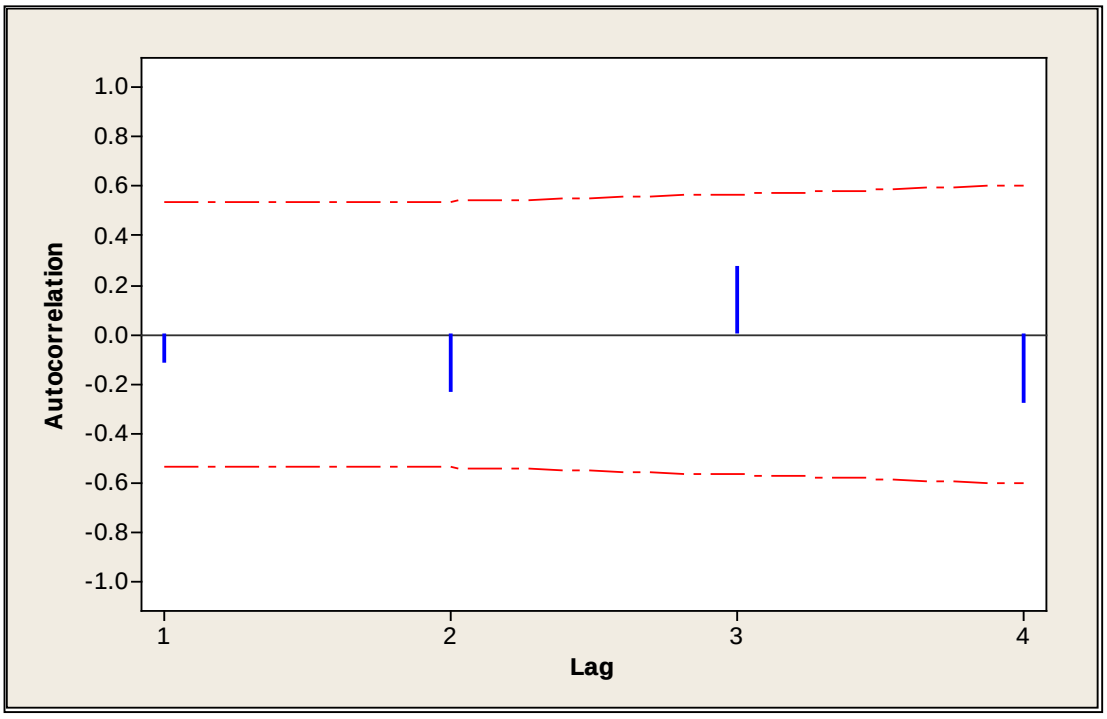

Figure A-13. ACF of the logarithmic values of I-131 air activity concentration for Yokosuka NB

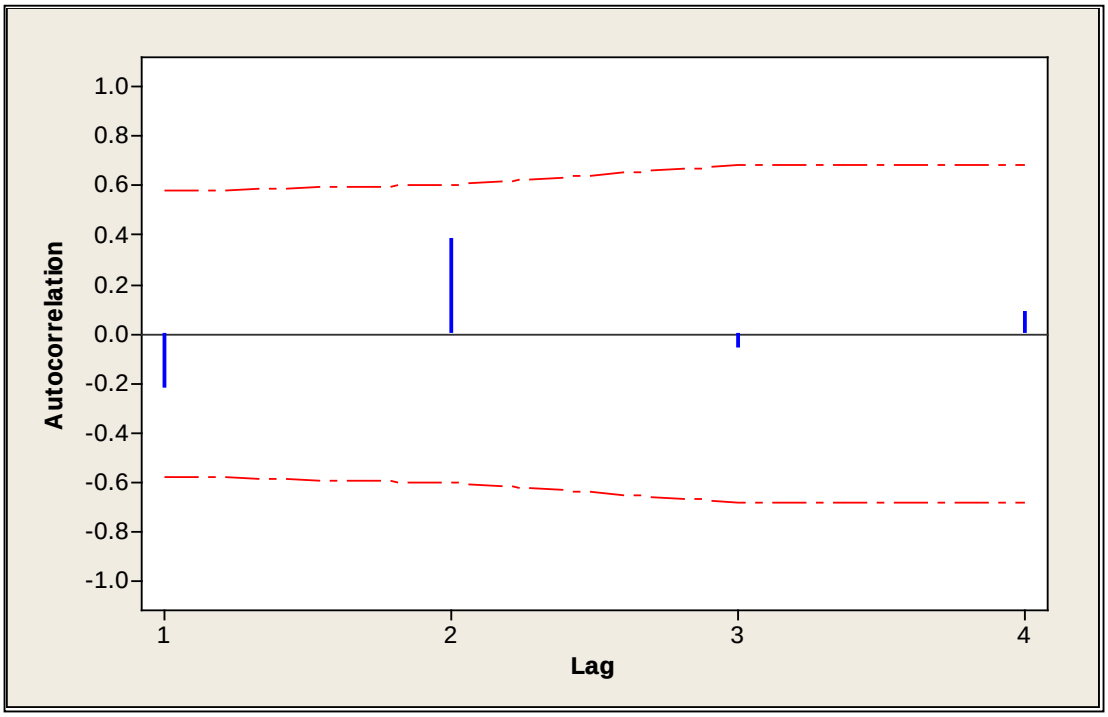

Figure A-14. ACF of the logarithmic values of Cs-134 air activity concentration for Yokosuka NB

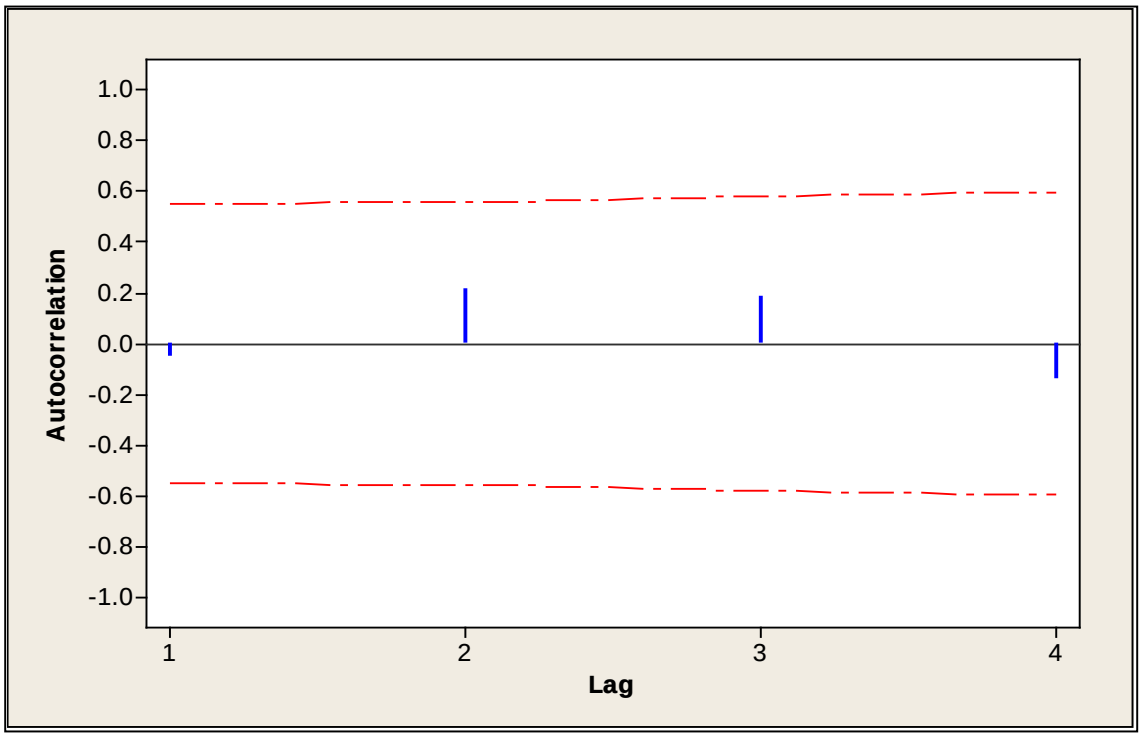

Figure A-15. ACF of the logarithmic values of Cs-137 air activity concentration for Yokosuka NB

A-3. First Differences

A-3.1. Iodine-131

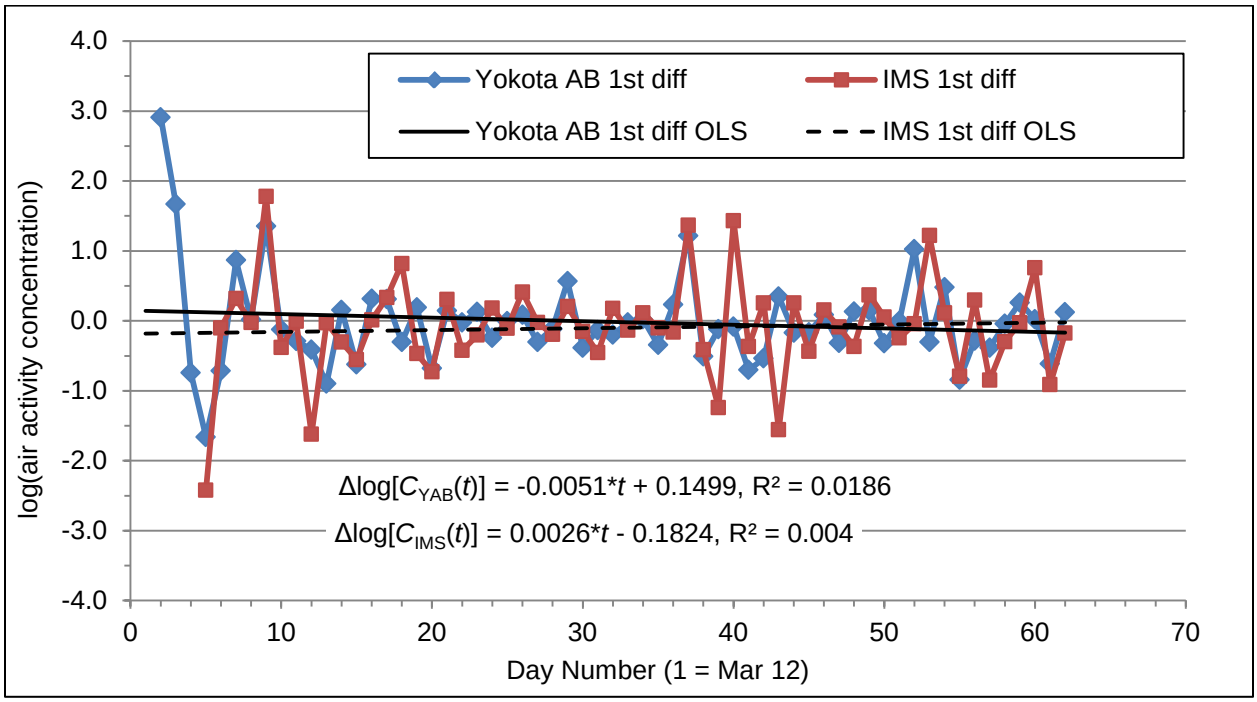

Figure A-16. First differences in logarithmic values of I-131 air activity concentration for Yokota AB and IMS-Takasaki

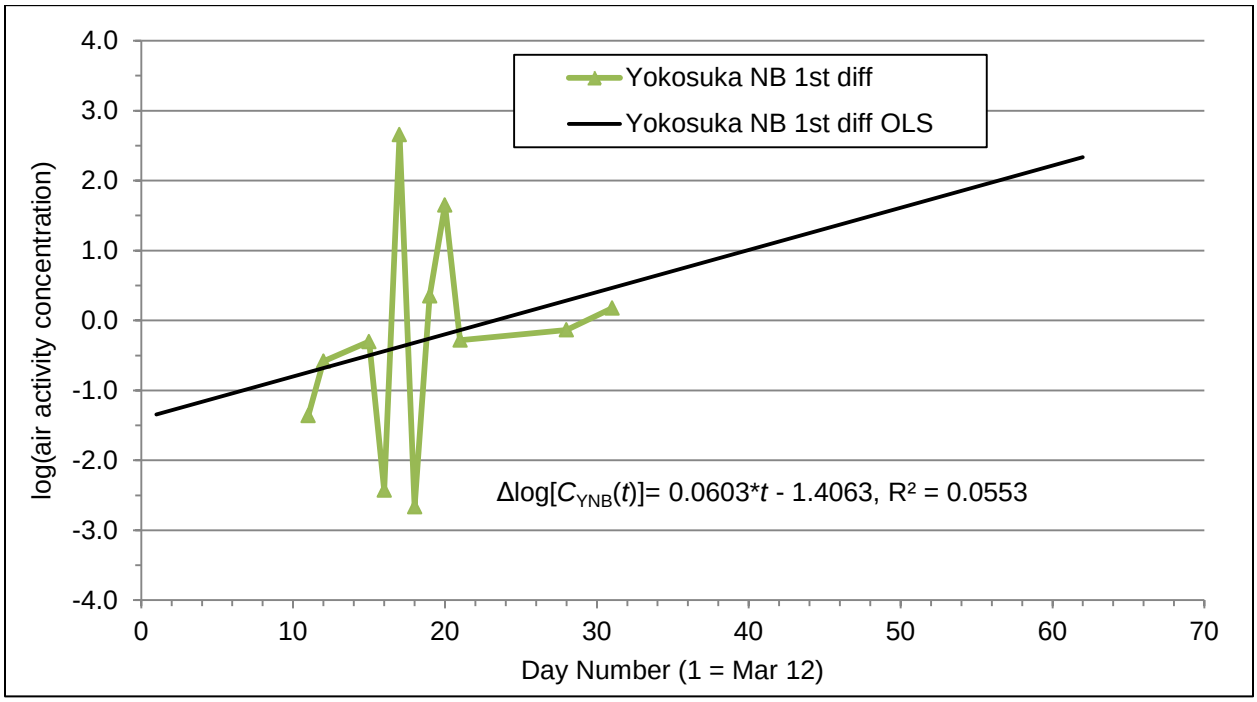

Figure A-17. First differences in logarithmic values of I-131 air activity concentration for Yokosuka NB

A-3.2. Cesium-134

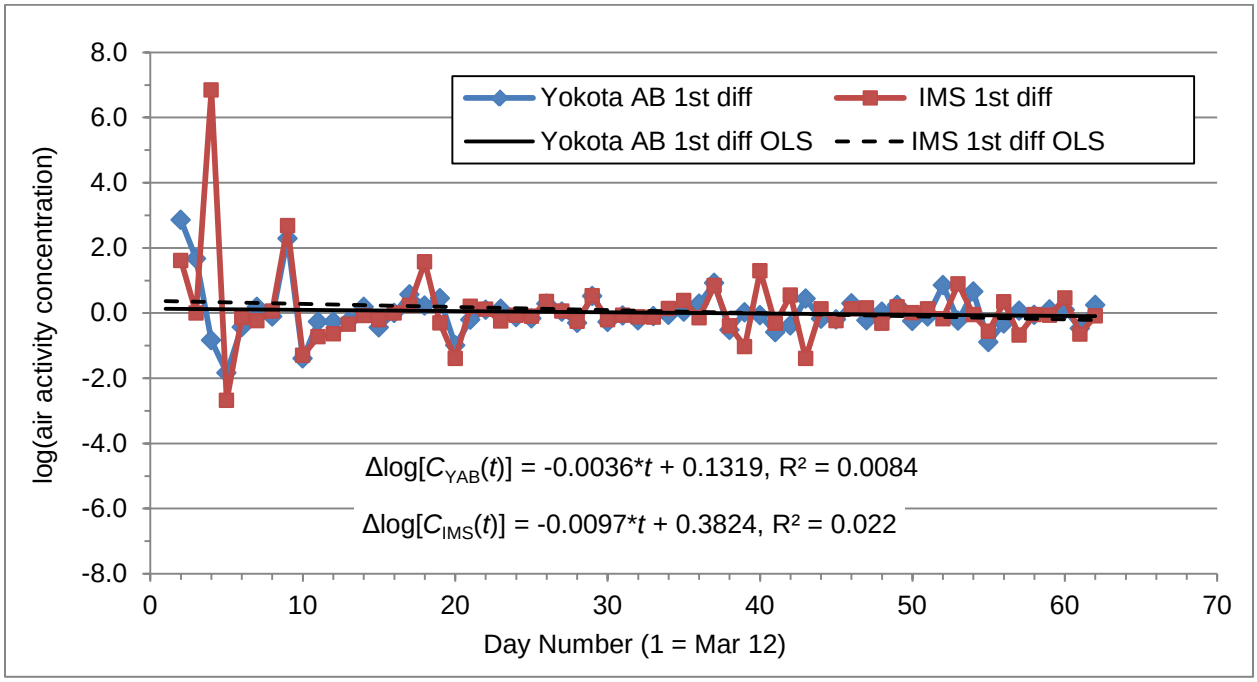

Figure A-18. First differences in logarithmic values of Cs-134 air activity concentration for Yokota AB and IMS-Takasaki

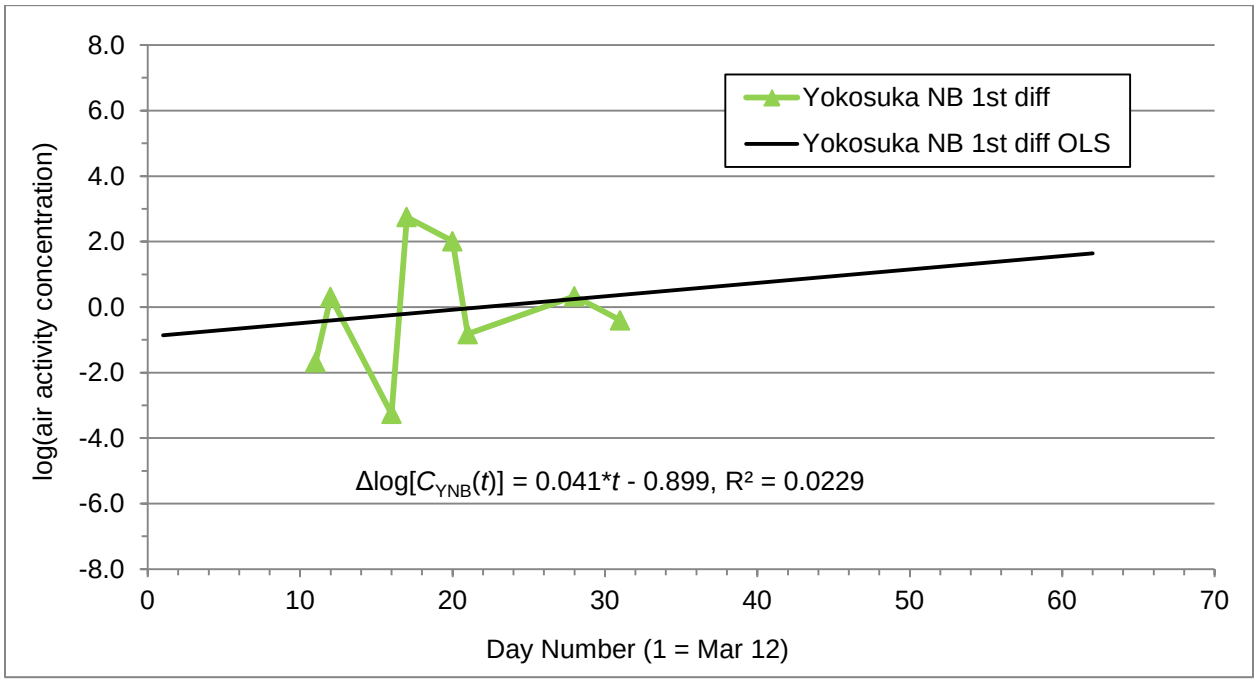

Figure A-19. First differences in logarithmic values of Cs-134 air activity concentration for Yokosuka NB

A-3.3. Cesium-137

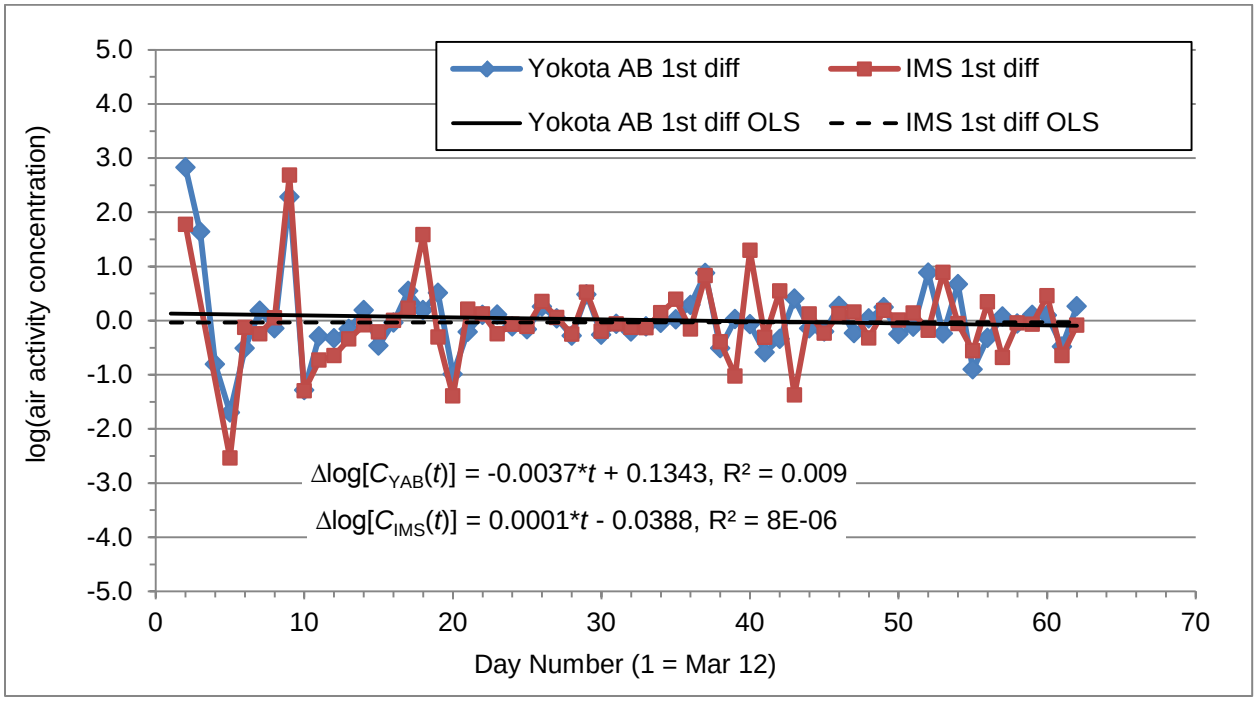

Figure A-20. First differences in logarithmic values of Cs-137 air activity concentration for Yokota AB and IMS-Takasaki

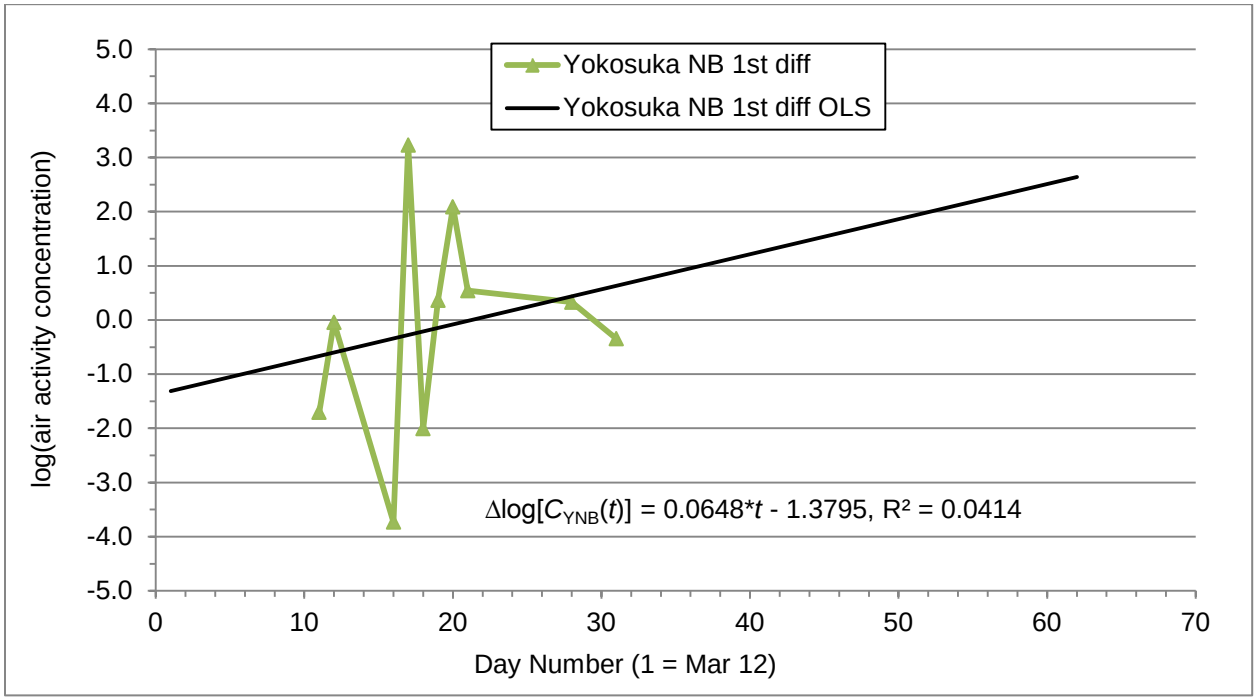

Figure A-21. First differences in logarithmic values of Cs-137 air activity concentration for Yokosuka NB

A-4. Cointegration

A-4.1. Iodine-131

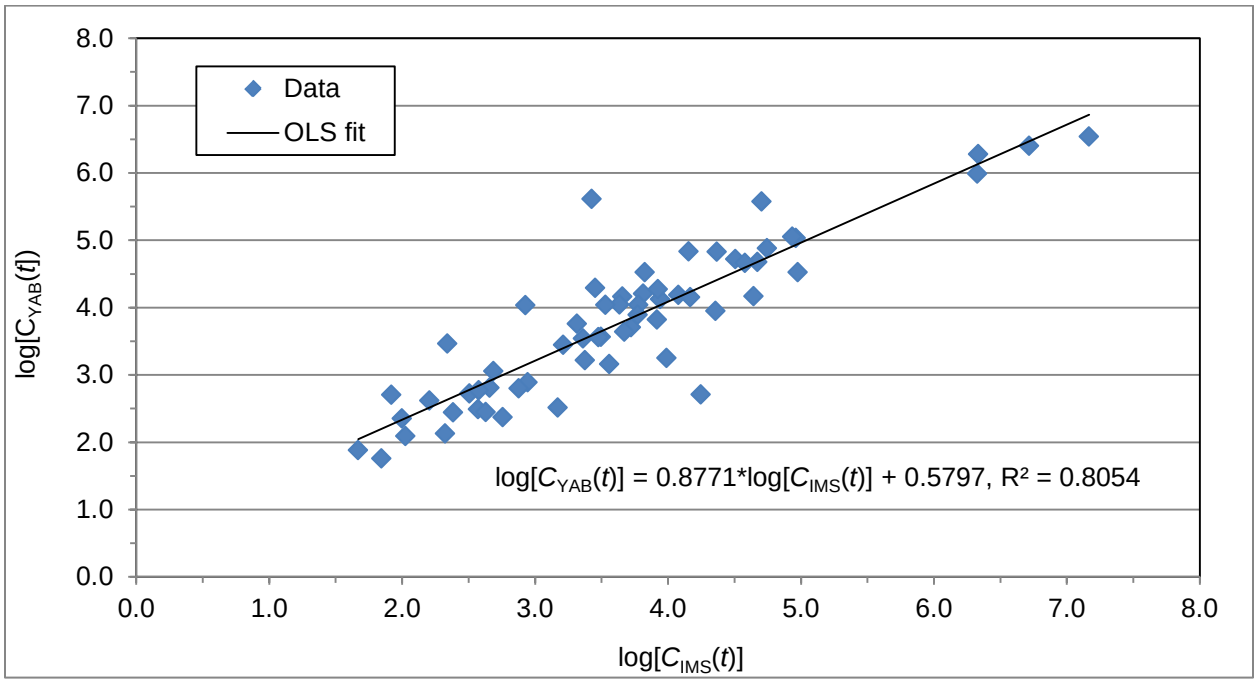

Figure A-22. Cointegrating OLS relationship between Yokota AB and IMS-Takasaki for I-131

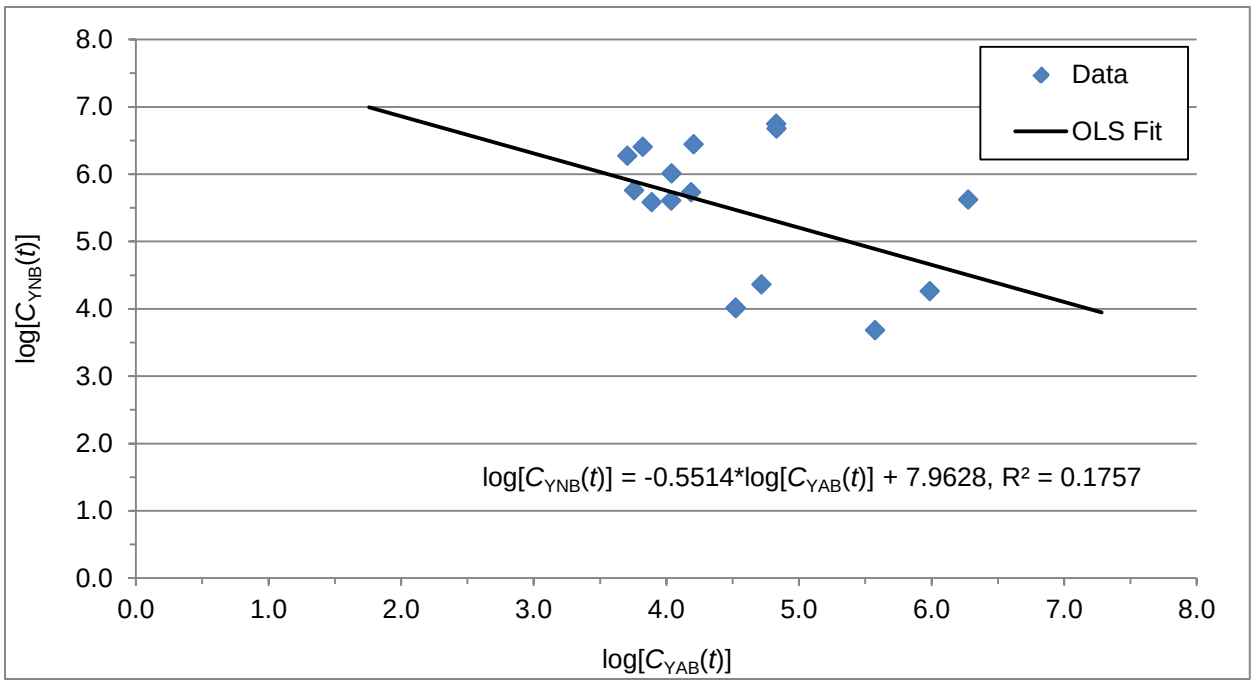

Figure A-23. Cointegrating OLS relationship between Yokosuka NB and Yokota AB for I-131

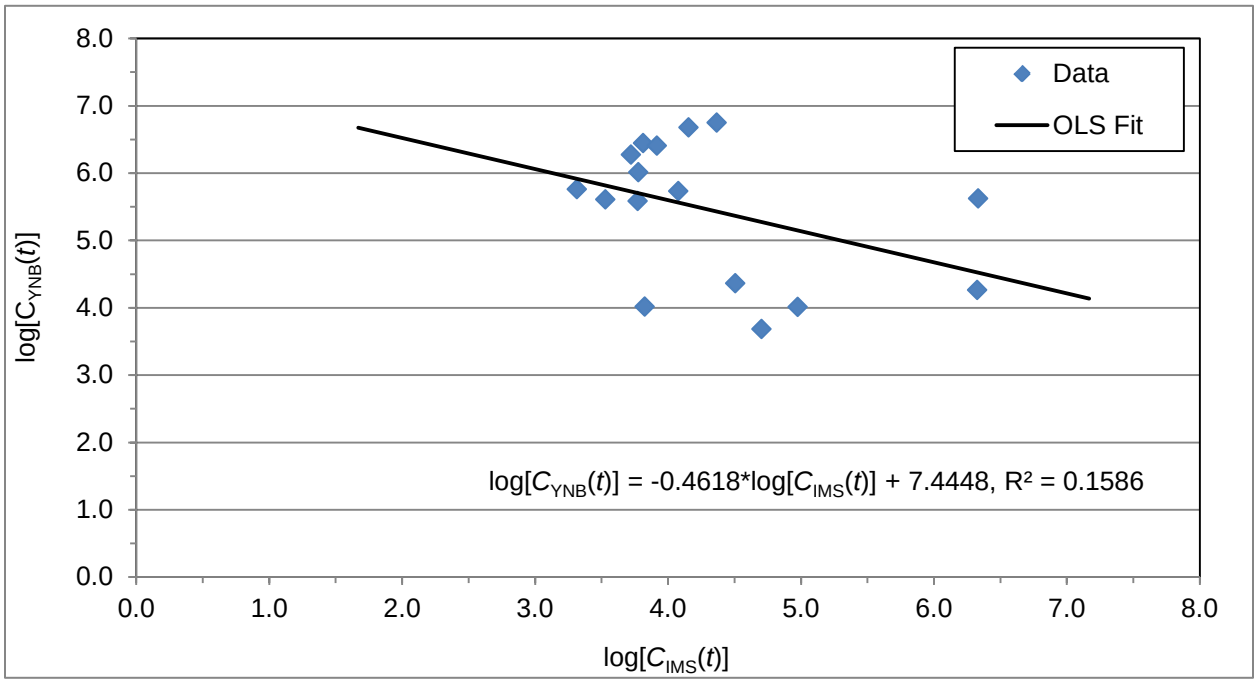

Figure A-24. Cointegrating OLS relationship between Yokosuka NB and IMS-Takasaki for I-131

A-4.2. Cesium-134

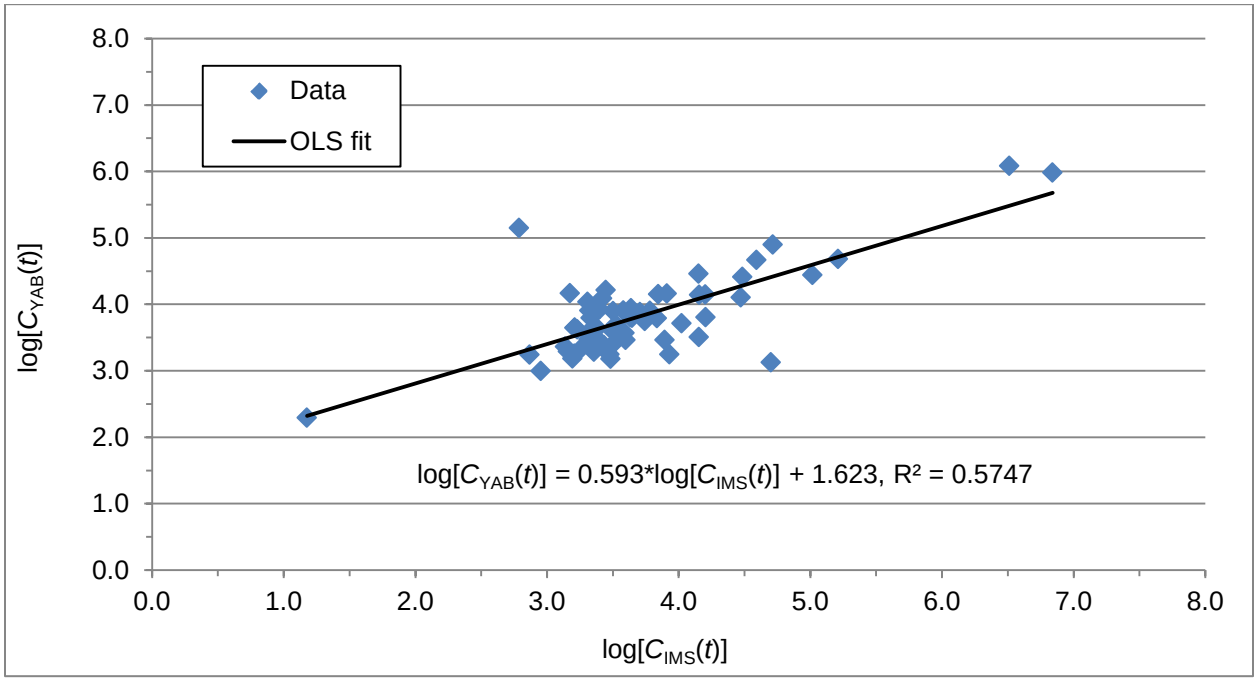

Figure A-25. Cointegrating OLS relationship between Yokota AB and IMS-Takasaki for Cs-134

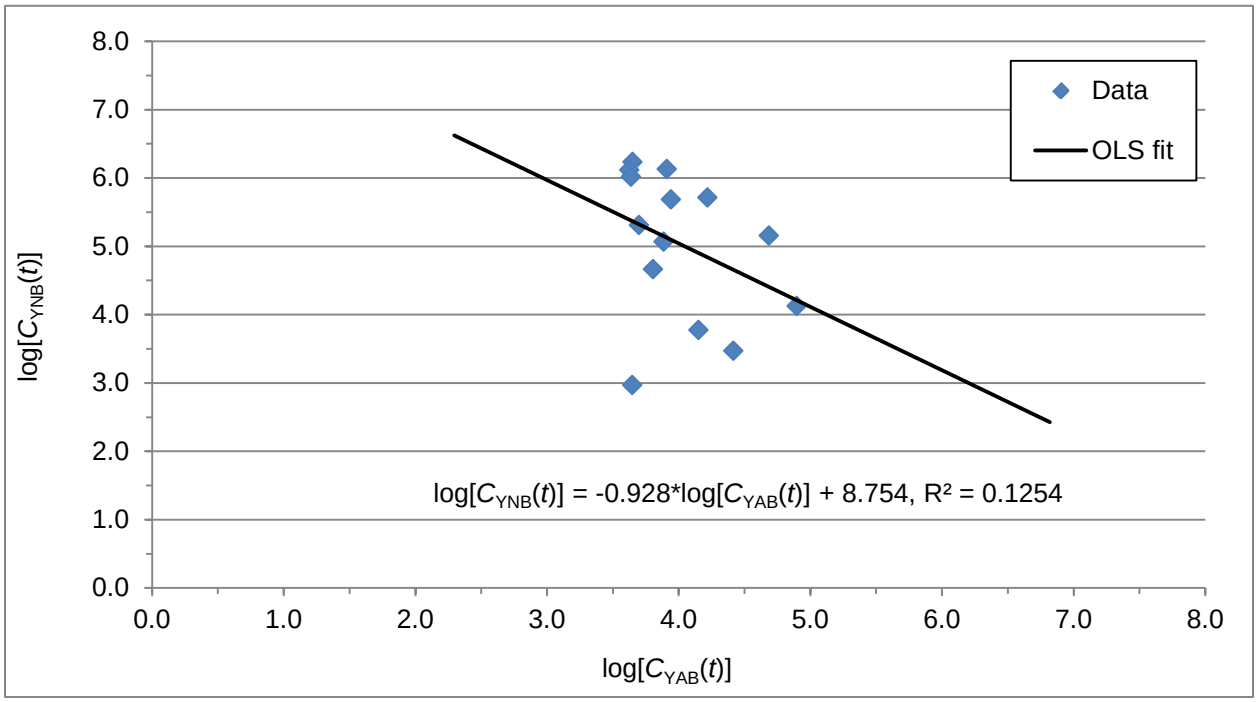

Figure A-26. Cointegrating OLS relationship between Yokosuka NB and Yokota AB for Cs-134

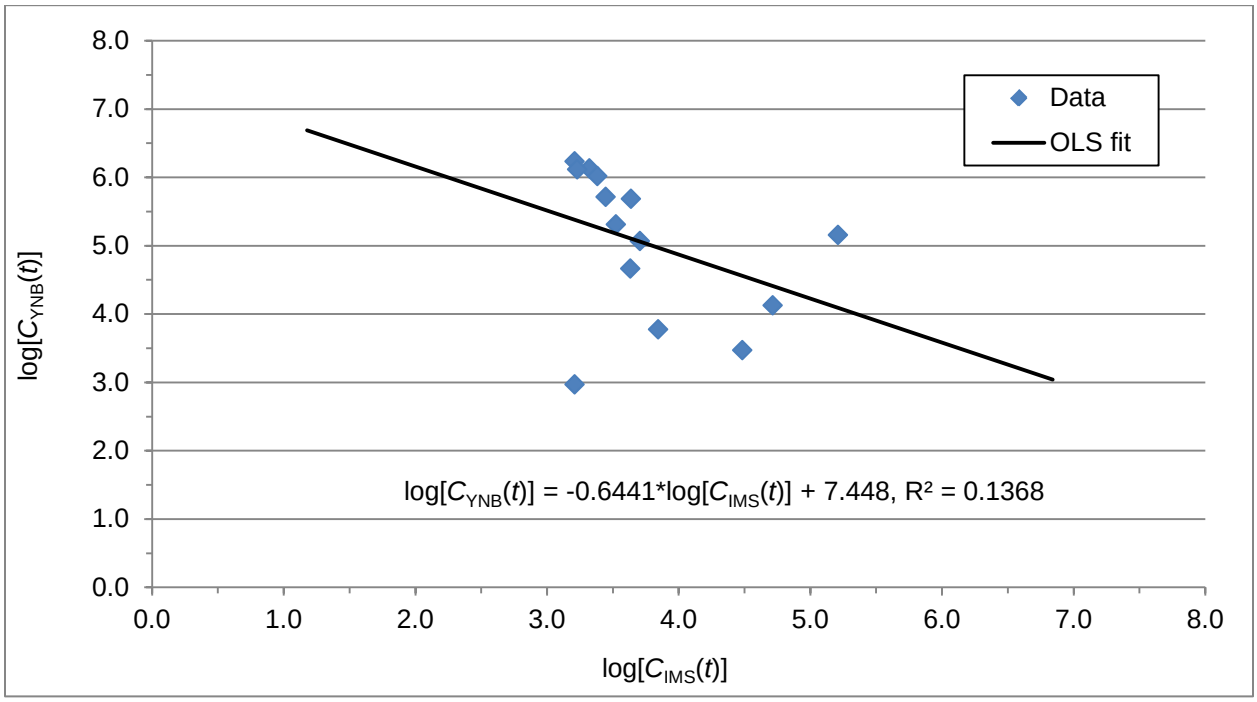

Figure A-27. Cointegrating OLS relationship between Yokosuka NB and IMS-Takasaki for Cs-134

A-4.3. Cesium-137

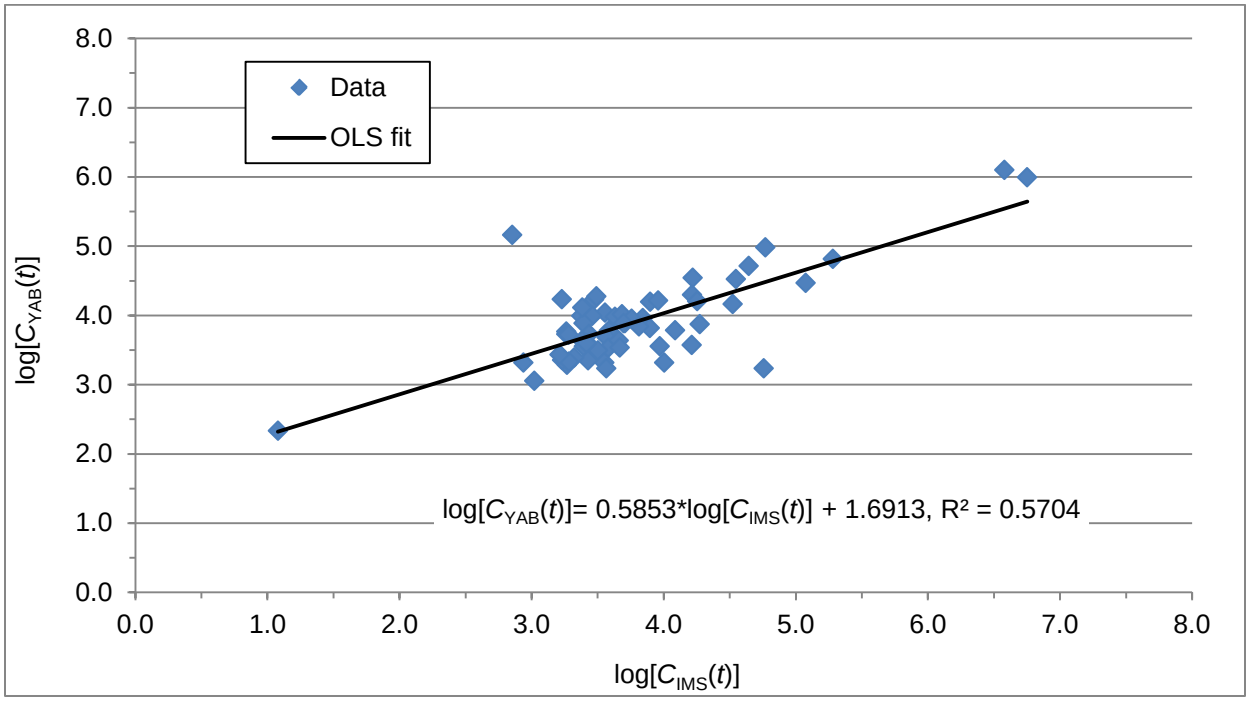

Figure A-28. Cointegrating OLS relationship between Yokota AB and IMS-Takasaki for Cs-137

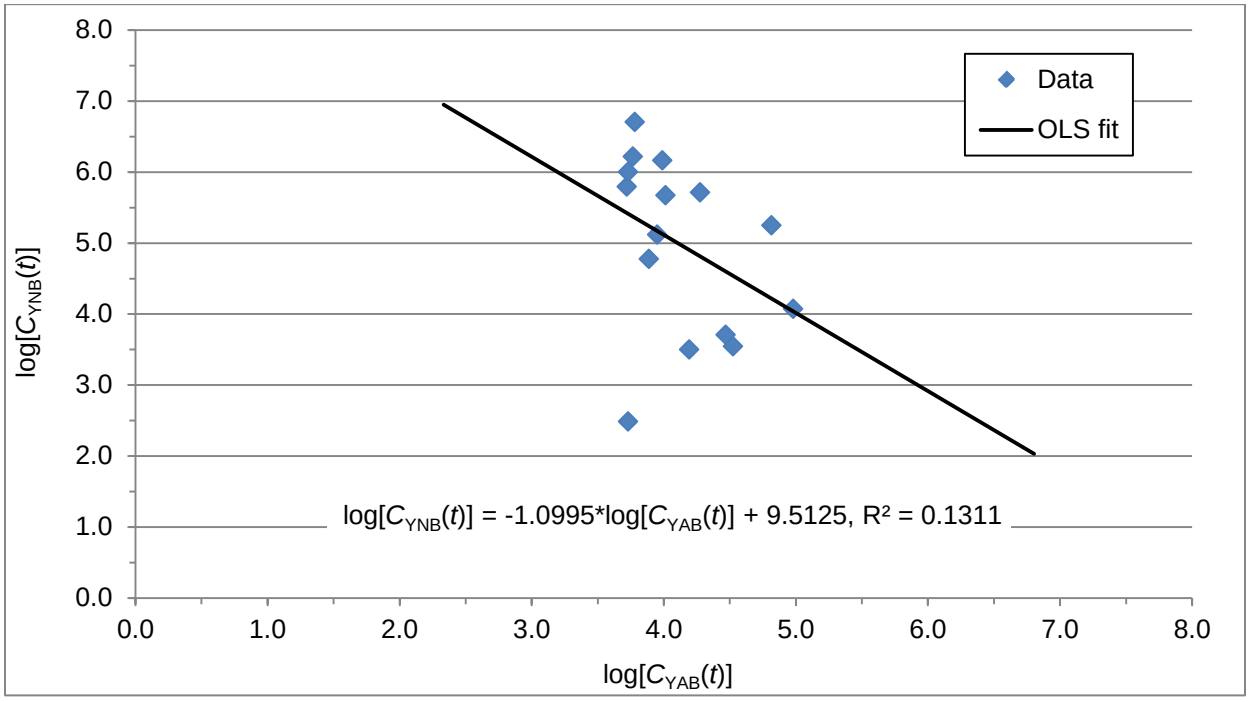

Figure A-29. Cointegrating OLS relationship between Yokosuka NB and Yokota AB for Cs-137

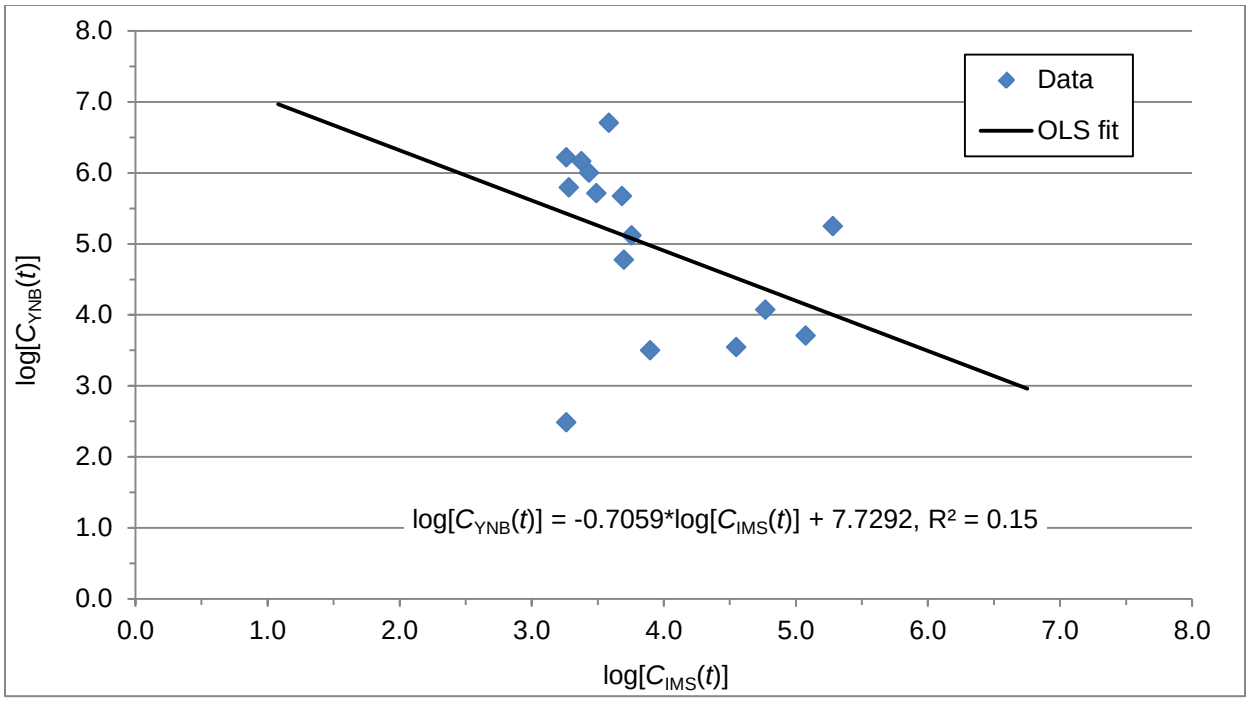

Figure A-30. Cointegrating OLS relationship between Yokosuka NB and IMS-Takasaki for Cs-137

A-5. Pairwise Differences

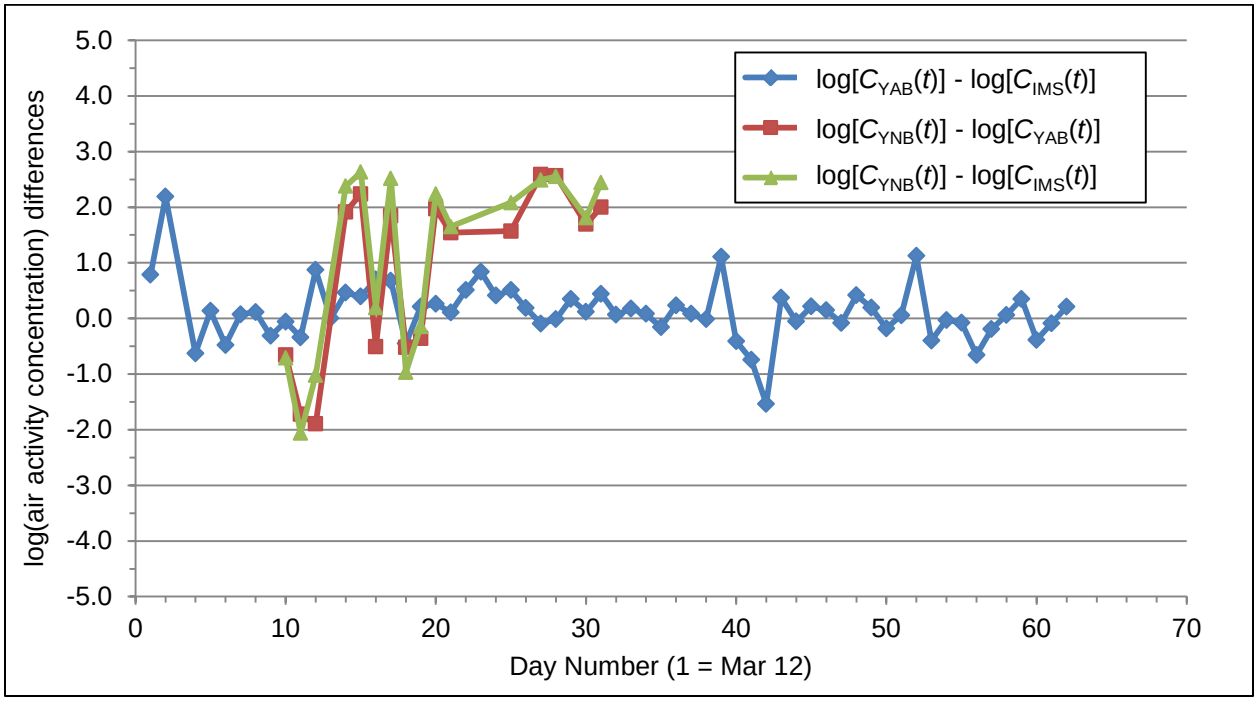

Figure A-31. Pairwise differences of the logarithmic values of air activity concentration for I-131

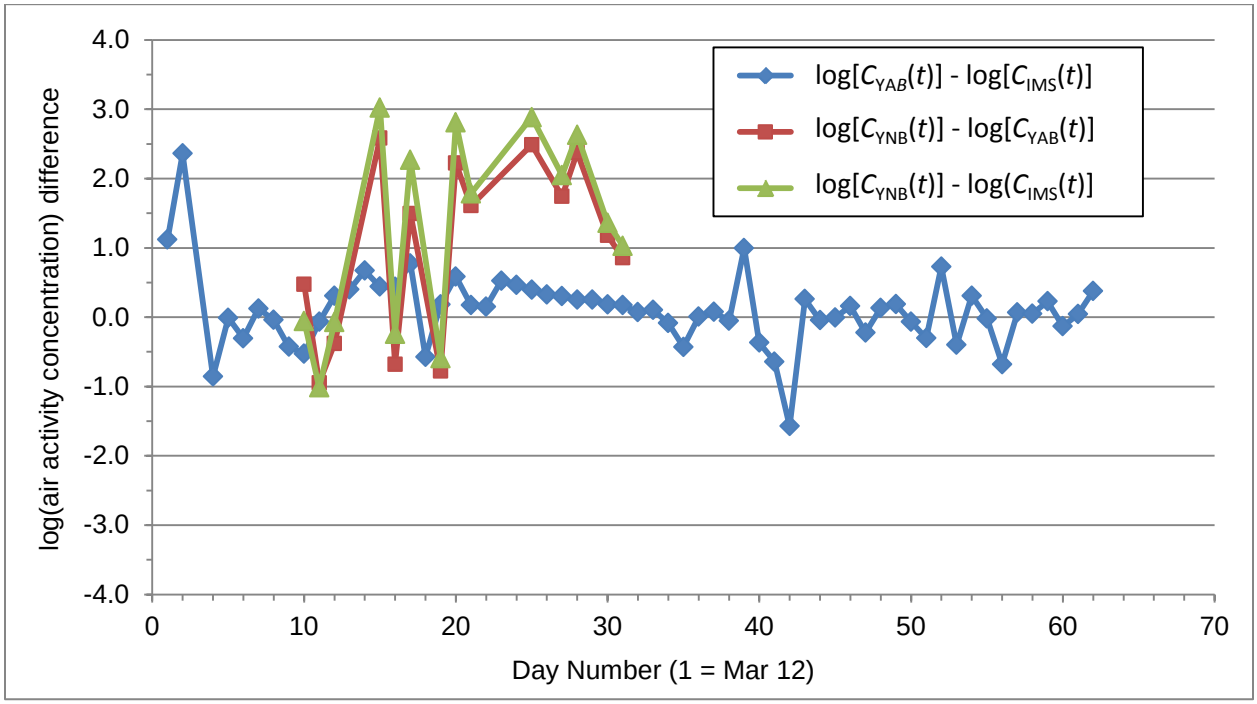

Figure A-32. Pairwise differences of the logarithmic values of air activity concentration for Cs-134

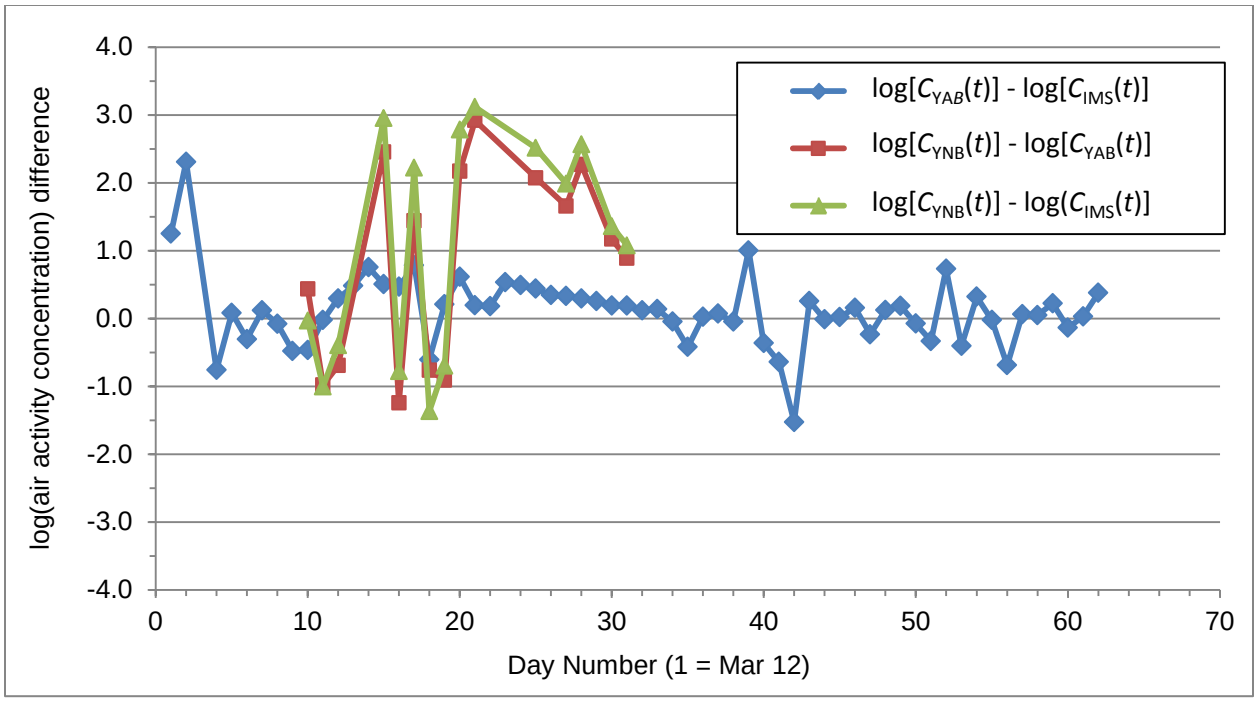

Figure A-33 . Pairwise differences of the logarithmic values of air activity concentration for Cs-137